Invited Review Paper

Forecasting of droughts and tree mortality under global warming: a review of causative mechanisms and modeling methods

Jeongwoo Han and Vijay P. Singh

ABSTRACT

Droughts of greater severity are expected to occur more frequently at larger space-time scales under global warming and climate change. Intensified drought and increased rainfall intermittency will heighten tree mortality. To mitigate drought-driven societal and environmental hazards, reliable long-term drought forecasting is critical. This review examines causative mechanisms for drought and tree mortality, and synthesizes stochastic, statistical, dynamical, and hybrid statistical-dynamical drought forecasting models as well as theoretical, empirical, and mechanistic tree mortality forecasting models. Since an increase in global mean temperature changes the strength of sea surface temperature (SST) teleconnections, forecasting models should have the flexibility to incorporate the varying causality of drought. Some of the statistical drought forecasting models, which have nonlinear and nonstationary natures, can be merged with dynamical models to compensate for their lack of stochastic structure in order to improve forecasting skills. Since tree mortality is mainly affected by a hydraulic failure under drought conditions, mechanistic forecasting models, due to their capacity to track the percentage of embolisms against available soil water, are adequate to forecast tree mortality. This study also elucidates approaches to improve long-term drought forecasting and regional tree mortality forecasting as a future outlook for drought studies.

Key words | causative mechanisms, drought, forecasting methods, global warming, soil degradation, tree mortality

Jeongwoo Han
Dept. of Biological and Agricultural Engineering,
Texas A & M University, TAMU,
College Station, TX 77843-2117,
USA

Vijay P. Singh (corresponding author)
Dept. of Biological and Agricultural Engineering
and Zachry Dept. of Civil and Environmental
Engineering,
Texas A & M University, TAMU,
College Station, TX 77843-2117,
USA
and
National Water Center,
UAE University,
Al Ain,
UAE
E-mail: *vsingh@tamu.edu*

INTRODUCTION

Drought is a recurring climatic phenomenon, initiated by below-normal precipitation persisting for an extended period (Mishra & Singh 2010; Dai 2011a; Hao & Singh 2015). Creeping nature and lingering effects of drought obscure the detection of the exact timing of initiation and termination of drought (Wilhite 2005; Hao & Singh 2015). In addition, intertwined causative physical processes and nonlinear feedbacks of the oceanic-atmospheric-land system manifest equivocal definition of drought (Kavvas & Anderson 1996). The lack of a universal definition of drought coined the conceptual framework of multistage drought propagation, based on hydroclimatic variables and the purpose of discipline (Mukherjee *et al.* 2018). Once initiated with a deficit of precipitation (meteorological drought), drought propagates into the depletion of soil moisture (agricultural drought), reduction of runoff (hydrologic drought), lowering of groundwater table (groundwater drought), and eventually socioeconomic disruption

doi: 10.2166/wcc.2020.239

(sociological drought) (Mishra & Singh 2010; Hao *et al.* 2018; Mukherjee *et al.* 2018).

Based on its intensity, duration, frequency, and areal extent, as well as regional hydrologic conditions, drought leads to the loss of agricultural productivity, reduced domestic water supply, lower industrial productivity, and disruption in the ecosystem (Mishra & Singh 2010; Hao *et al.* 2018). The drought-driven environmental and societal impacts can be aggravated by human population growth and the amplified water demand exceeding available water resources (D'Odorico *et al.* 2010). Drought, as the costliest natural disaster, has caused an average annual loss of $6–8 billion in the U.S. alone (FEMA 1995). The recent extreme drought of California (2011–2017) caused agricultural losses amounting to $5.5 billion and the destruction of 130 million trees (Kam *et al.* 2019). Besides the economic loss, drought contributes to tree die-off and deforestation, which in turn change forest to CO_2 emitter and influence climate and ecological degradation (McDowell *et al.* 2008; Allen *et al.* 2010).

Since drought occurrences are natural phenomena, which are beyond human control, proactive drought mitigation strategies aimed at drought resilience should be prioritized (Fu *et al.* 2013; Mukherjee *et al.* 2018). Decision/policy makers or stakeholders, therefore, need a robust proactive drought mitigation plan which relies on reliable monitoring, assessment, and forecasting of drought characteristics (Wilhite 2005; Nam *et al.* 2015). Given the complexity and equivocal definition of drought, the fundamental issues of drought monitoring and forecasting are the objective assessment and comparison of quantified droughts in time and space (Heim 2002; Wilhite 2005). To quantify drought, a compound measure, so-called drought index, that aggregates multiple drought indicators has been applied, such as Reconnaissance Drought Index (RDI), Standardized Precipitation Evaporation Index (SPEI), and Palmer Drought Severity Index (PDSI) (Palmer 1965; McKee *et al.* 1993; Mishra & Singh 2010; Vicente-Serrano *et al.* 2010; Hao & Singh 2015). Although drought assessment has improved along with the development of various drought indices, critical issues associated with climate change, data uncertainty, and defining the base period still exist in formulating drought indices (Trenberth *et al.* 2014; Mukherjee *et al.* 2018; Scheff 2018).

Drought forecasting has its foundation on the understanding of how drought indicators interact in oceanic-atmospheric-land circulation and how initial hydrological conditions affect the development of drought (Kavvas & Anderson 1996; Mishra & Singh 2011; Hao *et al.* 2018). Although it is difficult to generalize drought causative mechanisms for all seasons and over the entire globe, many studies have considered primary contributors to drought as ocean-atmospheric teleconnection, land-atmospheric feedbacks, and chaotic synoptic weather conditions (Cook *et al.* 2009; Sheffield & Wood 2012; Hoerling *et al.* 2014; Williams *et al.* 2015; Hao *et al.* 2018). For example, the Dust Bowl drought of the 1930s in the United States was initiated with the ocean-atmospheric teleconnection (La Niña) and then the land-atmospheric feedback aggravated and prolonged the drought (Cook *et al.* 2009, 2013). Within the California drought during 2011–2017, the drought event of 2013–2014 began with the ocean-atmospheric teleconnection (La Niña) and persisted with the internal atmospheric variability (stagnant anticyclone) (Seager *et al.* 2014; Swain *et al.* 2014; Kam *et al.* 2019). The 2012 Great Plains drought, referred to as a flash drought, was initiated by internal atmospheric variability or chaotic synoptic weather conditions (Hoerling *et al.* 2014; Hao *et al.* 2018).

Therefore, screening out unforecastable noise, establishing a statistically significant relationship of ocean-atmospheric teleconnection with regional hydroclimatic variables, and physically sound modeling of climate and hydrologic processes with high resolution are essential to improve drought forecasting skills (Mishra & Singh 2010; Wood *et al.* 2015; Hao *et al.* 2018). Based on the explored causative mechanisms, various types of forecasting methods, such as statistical, dynamic, and hybrid forecasting models, have been developed (Mishra & Singh 2010; Hao *et al.* 2018). However, dynamic models are not successful in long lead-time (longer than 1-month) forecasting and statistical models need to have the flexibility to adapt to a changing climate (Wood *et al.* 2015).

Climate change is attributed to natural variability or anthropogenic warming or compound effects of both (Yeh *et al.* 2018). However, it is now accepted that the increased level of greenhouse gases (GHG) has contributed to global warming (Dai 2011b; Fu & Feng 2014). Under global warming scenarios, it is expected that the background state of sea surface temperature (SST) changes, such that occurrences of ocean-atmospheric circulation are affected and the spatial variability of extreme hydrologic events increases along with

intensified land-atmospheric feedback (Dong & Sutton 2007; Mishra & Singh 2011; Yeh *et al.* 2018). Therefore, better drought forecasting under global warming requires nonstationary statistical modeling and dynamic models which have low sensitivity to initial boundary conditions and high resolution (Mishra & Singh 2011; Wood *et al.* 2015; Hao *et al.* 2018; Mukherjee *et al.* 2018).

The reduced rhizosphere water content and increased population of pests and pathogens under drought conditions influenced by global warming affect the physiology of trees which in turn leads to an increase in tree mortality and devastation of ecosystems (McDowell *et al.* 2008; Allen *et al.* 2010; Berg & Sheffield 2018). The increase in tree mortality rate, along with droughts under global warming, has led to the increased possibility of reduction of forest worldwide, as documented for forests of southern Europe and temperate and boreal forests of western North America (Allen *et al.* 2010). van Nieuwstadt & Sheil (2005) also found a relationship between the El Niño Southern Oscillation (ENSO) related drought and die-off of the tropical moist forests in Borneo. Tree die-off can alter ecosystem structures (e.g., root biomass and canopy height), functions (e.g., biodiversity and productivity), and fluxes (e.g., carbon sequestration and cycling and water flux) (Anderegg *et al.* 2016). Therefore, increased tree mortality changes regional climate and lowers biodiversity, net primary productivity, and productivity of commodities (Ciais *et al.* 2005; Bigler *et al.* 2006; McDowell *et al.* 2008). While the importance of understanding causative mechanisms of tree mortality under drought conditions and environmental implications of tree mortality has gained attention, poorly monitored data and the stochastic nature of tree mortality have increased uncertainty of forecasting of tree mortality (Anderegg *et al.* 2016). Besides the effect of drought on tree mortality, land degradation, which is caused by natural climate variability, and anthropogenic activities on irrigation, can predispose trees to die off by salinization which drives drought-like hydraulic tree failure (Munns 2002; D'Odorico *et al.* 2013; Kath *et al.* 2015). Therefore, understanding of tree die-off caused by soil degradation can explain extended tree mortality following the termination of severe drought events.

This paper aims to synthesize forecasting methods of both droughts and tree mortality, based on causative mechanisms and implications of global warming. The next section covers drought causative mechanisms and impacts of global warming on the causative mechanisms. This is followed by sections on, in sequential order, discussion of limitations and benefits of drought forecasting methods, tree mortality causative mechanisms and forecastability of tree mortality under global warming, effects of soil degradation on tree die-off, and discussion of future prospects for forecasts of droughts and tree mortality. The conclusion of this study is given in the last section. The list of acronyms used in this study and complementary discussions of the causative mechanisms of drought can be found in supplement file-1. Recent advances in drought indices and their benefit and limitations and more details related to drought forecast models are separately discussed in supplement file-2.

CAUSATIVE MECHANISMS FOR DROUGHT

The atmospheric moisture deficit, which is mainly associated with meteorological drought, is affected by the teleconnection of global SST anomalies and/or atmospheric internal variability (Newman *et al.* 2003; Mo & Schemm 2008; Hoerling *et al.* 2009; Sheffield & Wood 2012; Wang *et al.* 2014). In addition, land-atmospheric feedbacks can accelerate the development or propagation of drought, once the meteorological drought occurred (Cook *et al.* 2009; Sheffield & Wood 2012; Hoerling *et al.* 2014; Williams *et al.* 2015). Drought causative mechanisms, in reality, cannot be dichotomized into quasi-periodic (contribution of SSTs) and less forecastable components (effects of random atmospheric internal variability and land-atmosphere feedback). However, to understand the process of drought development, this study divides the intertwined causative physical processes into anomalies of SST, atmospheric internal variability, and land-atmosphere feedbacks, and discusses each causative mechanism and its interaction (Mishra & Singh 2010; Sheffield & Wood 2012; Hao *et al.* 2018).

Anomalies of sea surface temperature (SST) and their role

Since atmospheric flows are critical moisture supply channels from oceans to inland areas, understanding of how anomalies of SST force ocean-atmospheric circulation

and regional hydroclimate are associated with drought is important. The ocean-atmospheric dynamics, which are induced by SST anomalies, are represented by ENSO, Pacific Decadal Oscillation (PDO), North Atlantic Oscillation (NAO), Arctic Oscillation (AO), Atlantic Multidecadal Oscillation (AMO), and Indian Ocean Dipole (IOD) (Enfield *et al.* 2001; Newman *et al.* 2003; Mo & Schemm 2008; Sheffield & Wood 2012).

ENSO is one of the most important driving forces which modulates interannual climate variability across most of the globe, including North America and South America, Australia, India, east and south Africa, and Southeast Asia (Sheffield & Wood 2012; Hao *et al.* 2018; Yeh *et al.* 2018). The impact of ENSO on droughts is shown in Figure 1. The mean of 3-month Standardized Precipitation-Evaporation Index (SPEI3) for February and the mean of 9-month SPEI (SPEI9) for August were estimated across the globe during ENSO's warm (El Niño) and cold (La Niña) years for the period of 1901–2006 (Figure 1; Beguería *et al.* 2010). The differences between El Niño and La Niña years are remarkable across most of the globe, and it is confirmed that ENSO has implications for the interannual variation of local terrestrial water budgets.

The occurrence of ENSO is linked to the tropical Pacific thermocline and the Walker circulation, which are modulated by the east-west thermal gradient over the tropical Pacific (Kumar *et al.* 1999; Sheffield & Wood 2012; Yeh *et al.* 2018). As El Niño matures, warm temperature in the western tropical Pacific expands toward the east of the tropical Pacific, such that the location of occurrence of deep atmospheric convection shifts to the central or eastern tropical Pacific (Cai *et al.* 2015; Yeh *et al.* 2018). In contrast, La Niña events mature by the process reverse of the El Niño occurrence. During the El Niño event, the western tropical Pacific has a subsided precipitation producing tendency, such that Australia, East Asia, the Maritime Continent, and east and south Africa, are prone to dryness (Schubert *et al.* 2016; Hao *et al.* 2018). In addition, interactions of El Niño along with IOD, PDO, and NAO have impacts on the strength of teleconnection outward from tropical areas and modulate the Indian monsoon and the East Asian monsoon which are critical moisture suppliers for India and Southeast Asia, respectively (Kumar *et al.* 1999; Xiao *et al.* 2015). For droughts in North America, ENSO, PDO, and AMO have salient implications (McCabe *et al.* 2004, 2007; Mo & Schemm 2008; Cook *et al.* 2014). Reduced winter precipitation in the southwestern U.S. and the western Great Plains have a significant correlation with La Niña (Seager *et al.* 2005; Cook *et al.* 2009). The positive phase of PDO impacts dryness (wetness) in the northwestern (southwestern) U.S. (McCabe & Dettinger 1999; Cook *et al.* 2014). The positive phase of the AMO induces dryness in the Midwest and southwest of the U.S. (Enfield *et al.* 2001; Sheffield & Wood 2012). However, the level of significance of

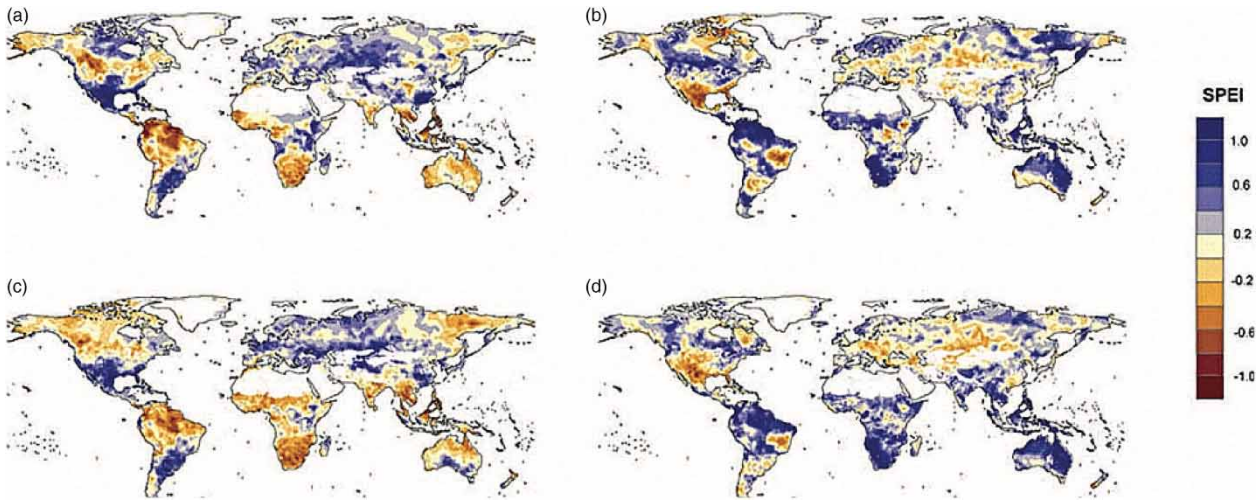

Figure 1 | Impact of ENSO on SPEI at the global scale: (a) Mean SPEI3 for February during El Niño years; (b) same with (a) but during La Niña years; (c) Mean SPEI9 for August during El Niño years; and (d) same with (c) but during La Niña years (Beguería *et al.* 2010).

ocean-atmospheric teleconnection to the U.S. is influenced by the combined effect of ENSO, PDO, and AMO which have different periodic spans, such as interannual, decadal, and multidecadal, respectively (McCabe & Dettinger 1999; Enfield *et al.* 2001; Dong *et al.* 2006; McCabe *et al.* 2007).

The variability of ENSO (i.e., amplitudes and asymmetry of El Niño and La Niña) are affected by SST anomalies of the North Atlantic Ocean via atmospheric and oceanic teleconnection (Dong *et al.* 2006; Dong & Sutton 2007). The negative SST anomaly over the tropical North Atlantic Ocean shifts the Atlantic intertropical convergence zone (ITCZ) southward and develops an anticyclonic circulation over midlatitude North Atlantic Ocean and increases northeast trade winds (Dong & Sutton 2007). As a consequence, interhemispheric SST dipole becomes prominent and, in turn, the east Pacific Ocean shows similar dipole patterns (cold and warm SST for the northern and southern hemisphere, respectively) such that northeasterly winds are reinforced (Dong & Sutton 2007; Yeh *et al.* 2018). The northeasterly wind anomalies shift the center of atmospheric deep convection over the tropical Pacific Ocean and contribute to the change in the Rossby waves which affect weather conditions by shifting midlatitude storm tracks, and modulate the ENSO teleconnection to regions outside of the tropics (McCabe & Dettinger 1999; Dong & Sutton 2007; Yeh *et al.* 2018). Therefore, during the cold phase of the North Atlantic Ocean, the El Niño teleconnection may be weakened and may show less significant correlation with precipitation in inland areas. Furthermore, PDO also modulates the strength of ENSO teleconnections by reinforcing El Niño (La Niña) anomalies when PDO is in a warm (cold) phase (McCabe & Dettinger 1999; Yeh *et al.* 2018).

Although PDO or AMO themselves correlate with precipitation at decadal-to-multidecadal time scales, their interplay with ENSO may provide additional clues to understand the SST teleconnection to hydroclimate and improve drought forecasting skills (Hoerling *et al.* 2009). However, since the strength of SST teleconnection varies as global mean temperature increases, an understanding of the potential change in SST teleconnections under climate change will provide clues to improve drought forecasting methods. Therefore, we discuss details on the implications of global warming on SST teleconnection in Appendix 1B of supplement file-1. Since land-atmospheric feedback and internal atmospheric variability contribute to drought occurrence and its development, we will discuss their impacts on drought in the following section.

Land-atmospheric feedback and internal atmospheric variability and their role

Land-atmospheric feedback

Aerosols (e.g., dust, sea salt, and volcanic ash) and land surface changes affect the weather and climate of the Earth by aerosol-radiation interaction (ARI) mechanism (Cook *et al.* 2013; Li *et al.* 2017): When wind-blown dust aerosols are amplified with increases of bare soil, the aerosols directly reflect incoming shortwave solar radiation and reduce the downwelling energy reaching the terrestrial surface, such that the energy deficit is magnified (Donohoe & Battisti 2011; Cook *et al.* 2013). The increased energy deficit stabilizes the land-atmospheric dynamics and, in turn, the dry condition is prone to occur by inhibited convection (Cook *et al.* 2013). The iconic drought event related to land-atmospheric feedbacks is the Dust Bowl drought of the 1930s across the central U.S. Great Plains (Cook *et al.* 2009, 2013; Sheffield & Wood 2012). The Dust Bowl drought was initiated with below-normal precipitation caused by the La Niña event and, in turn, the drought-sensitive crops were withered at the early stage of the drought and the farmland was degraded into barren which is easily eroded by winds (Worster 2004; Cook *et al.* 2009).

Cook *et al.* (2009) disclosed land-atmospheric feedback mechanisms through the Dust Bowl drought. They assessed the effects of each isolated factor (SST, Crop failure (hereafter Crop), and Dust amplification (hereafter Dust)) on precipitation and temperature that were hindcasted by the Goddard Institute for Space Studies atmospheric general circulation model (GCM) (GISS ModelE) for the period of 1932–1939. Anomalies of the hindcasted precipitation and temperature, which were affected by the isolated factors, were compared with anomalies of Climate Research Unit Time-Series version 2.1 (CRU TS2.1) considered as true observation (Figures S1-1 and S1-2 in Appendix 1C of supplement file-1). Adding a single factor (Crop or Dust) to SST could not reproduce the patterns of precipitation and temperature of the Dust Bowl drought, but adding all

the factors mimicked those well (for details, see Appendix 1C in supplement file-1). For more details on the effects of land-atmospheric feedback mechanisms for the Dust Bowl drought, reference is made to Cook *et al.* (2009).

The land-atmospheric feedback mechanisms explained for the Dust Bowl drought might be applicable for the Medieval Climate Anomalies (circa 1,100–1,500 Common Era) which caused megadrought (lasting for a decade or multidecade) in the western North and central Great Plains (Cook *et al.* 2009, 2013, 2014). The paleoclimate showed that the dune mobility and continuous changes of land geomorphology occurred due to the destabilized soil, implying complete loss of vegetation during that era (Cook *et al.* 2009, 2013).

Internal atmospheric variability

Drought can be more severe and more prolonged due to internal atmospheric variability which shifts the location of jet stream and mid-latitude storm tracks and affects zonal atmospheric anomalies (Harzallah & Sadourny 1995; Liu & Alexander 2007; Wang *et al.* 2014). A Rossby wave, known as an atmospheric bridge, is initially formed by SST anomalies and propagates energy waves from west to east inside wave guards/boundaries by meandering between ridge and trough of atmospheric pressure (Figure S1–3(b) in Appendix 1D of supplement file-1) (Hoskins & Ambrizzi 1993; Wang *et al.* 2014). The atmospheric internal variability can amplify the Rossby wave and elongate its persistence. The extreme drought in California during 2013–2014 was caused by the shifting of the jet stream to the north and blocking of moisture flow into the west coast of the U.S due to the long-lasting ridge, which was caused by the abnormal Rossby wave over the eastern Pacific (for details see Appendix 1D in supplement file-1). As a consequence, it led to the lowest precipitation amounts, which were around 10% of the normal (the ratio to the climatology; right-side map of Figure S1–3(b) in Appendix 1D of supplement file-1), in the last 119-year observations and caused the extreme drought event in California (Seager *et al.* 2014; Swain *et al.* 2014; Wang *et al.* 2014; Wang & Schubert 2014; Williams *et al.* 2015).

Based on the causative mechanisms of drought reviewed thus far, it is expected that skillful drought forecasting can be accomplished by answering the questions as follows: How significantly the correlation between SST teleconnections and hydroclimate variables in inland areas is established; how the nonlinear or chaotic nature of internal atmospheric variability can be incorporated in forecasting models; and how accurately land-atmosphere feedback can be simulated by hydrological or land surface model. Besides, understanding the causative mechanisms of drought and implications of global warming for them suggests the nonstationary nature of drought into drought forecasting.

DROUGHT FORECASTING METHODS

Before discussing drought forecasting methods, drought quantification methods, developed during the last decades, are synthesized, and their advantages and limitations are discussed (See Appendix 2A of supplement file-2). Drought forecasting has its foundation in establishing a significant relationship between drought and drought indicators and/or finding seasonal or periodic patterns of drought (Hao *et al.* 2018). When we consider the nonstationarity of drought under global warming discussed in previous sections, it is expected that drought forecasting methods need to consider the non-static drought causative mechanisms. Some issues in considering drought mechanisms into modeling frameworks are discussed in Appendix 2B of supplement file-2. Although various statistical, dynamical, and hybrid drought forecasting models have been developed, the ability of forecasting models to consider the evolutionary drought causative mechanisms and chaotic atmospheric variation is still a question (Mishra & Singh 2011; Hao *et al.* 2018; Fung *et al.* 2019). Since drought is characterized by its severity, duration, interarrival time, and areal extent, how well forecasting models forecast the characteristics of drought is a key to successful drought mitigation planning (Mishra & Singh 2011). Temporal aspects of drought characteristics, such as severity, duration, and interarrival time, can be quantified by applying the theory of runs (Yevjevich 1967; Kendall & Dracup 1992; Mishra & Singh 2011). The areal extent of the temporal aspects of drought characteristics is estimated by spatial interpolation (Akhtari *et al.* 2009). When, on the other hand, the regionalization of a drought index is already accomplished by using a climate model and a distributed hydrological model, the theory of run can be applied to each cell/grid to define drought characteristics therein

(Rajsekhar *et al.* 2015). From the perspective of forecasting drought characteristics, methodological approaches can be distinguished into two frameworks: (1) to use directly historical observations of severity and drought occurrence in the forecasting process (hereafter referred to as prior-application of the theory of runs), and (2) to apply the theory of runs after forecasting drought index (hereafter referred to as post-application of the theory of runs). Therefore, we synthesize drought forecasting methods, including stochastic (to emphasize models of probabilistic nature), statistical, dynamical, and hybrid models, in these two forecasting frameworks.

Prior-application of the theory of runs

The theory of runs differentiates drought conditions into two states (dry and wet conditions) or multiple states (e.g., severe drought, moderate drought, normal, moderate wet, and severe wet) based on the number of thresholds one applies (Lohani & Loganathan 1997; Chung & Salas 2000; Mishra *et al.* 2009; Hao *et al.* 2018). Figure S2-1 in Appendix 2C of supplement file-2 depicts temporal aspects of drought characteristics after applying the theory of runs (see details in Appendix 2C of supplement file-2). Several stochastic models have been widely used in this forecasting approach. Markov chain (MC) models (Lohani & Loganathan 1997; Cancelliere *et al.* 2007; Avilés *et al.* 2015), and discrete autoregressive moving average (DARMA) models (Chung & Salas 2000) have been widely used to forecast duration and interarrival time for drought early warning. The alternating renewal-reward (ARR) model (Kendall & Dracup 1992; Mishra *et al.* 2009) can be used to forecast duration, interarrival time, and severity simultaneously.

Stochastic drought forecasting models

Markov chain (MC) models. Stochastic evolution of countable states (two states or multiple states) is simulated by MC models governed by the transition probability matrix (Lohani & Loganathan 1997; Avilés *et al.* 2015). MC models forecast the state of the next time (S_{t+1}) by depending on the current known state (S_t) in the case of first-order MC (Lohani & Loganathan 1997). Therefore, the transition probability is represented by a conditional probability. The mathematical expression of MC models can be found in Appendix 2D of supplement file-2. The MC model can be extended to the higher-order model which can depend on the current and previous times (i.e., second-order MC) (Avilés *et al.* 2015; Hao *et al.* 2018). Lohani & Loganathan (1997) forecasted the state of drought at the 4-month lead time by using monthly PDSI such that drought onset, termination, or persistence can be inferred with the probability of its occurrence. They used a non-homogeneous first-order MC model to consider monthly variation or cyclic patterns of PDSI, and decision tree analysis to track the transition of drought from the current to the target month. The forecasted drought occurrences were coincident with the observed drought events. Avilés *et al.* (2015) used an Aggregate Drought Index (ADI), which combines multiple hydrologic variables by using principal component analysis (PCA), in the first-order and the second-order MC models. They also used decision tree analysis and forecasted drought state for 3 months (DJF) that has the highest frequency of drought occurrence in the Chulco River basin in southern Ecuador. The second (first)-order MC models showed 47% (30%) of the hit rate, and both models had a false alarm rate of less than 10%.

However, the estimation of the transition matrix is significantly affected by the length of observation due to too insufficient samples to reliably estimate the frequency of transitions, especially for multistate drought (Cancelliere *et al.* 2007). In this context, Cancelliere *et al.* (2007) estimated the transition matrix using an analytical method based on the autocovariance of Standardized Precipitation Index (SPI) and compared it with the empirically estimated transition matrix. They showed that the analytically-driven transition matrix resulted in better forecasting than the empirically-driven one. Besides, MC models use a short-term dependency which, in turn, may lose long-term self-dependency of drought (Chung & Salas 2000).

Discrete autoregressive moving average (DARMA) models. Most of the hydrologic variables, which have sub-annual temporal scales, show a certain degree of autocorrelation which, in turn, makes MC models ineligible (Chung & Salas 2000). However, Discrete Autoregressive Moving Average (DARMA) models can be used for drought forecasting even when an ordinal time series is highly autocorrelated (Jacobs & Lewis 1977; Chung & Salas 2000;

Sharma & Panu 2012). As a discrete version of autoregressive moving average (ARMA) models, DARMA models consider the persistence of time series of ordinal variables (e.g., drought = 0 and wetness = 1 which are defined by cutting off a drought index at a designated threshold) such that duration and its reliability are forecasted (Chung & Salas 2000; Cancelliere & Salas 2010; Sharma & Panu 2012). Low-order DARMA models have been used in drought forecasting. The mathematical theory of DARMA is explained in Appendix 2D of supplement file-2.

Chung & Salas (2000) forecasted occurrence times and interarrival times of droughts which have different durations varying from 1 to 12 years for the Niger River at Koulikoro in Africa and the South Platte River at Denver in the U.S. When the duration length is greater than 5 years, the estimated drought occurrence probability and interarrival time significantly deviate from historical observations due to not enough sub-samples for reliable historical estimation. Sharma & Panu (2012) estimated the transition probability matrices by using empirical and Discrete Autoregressive (DAR) (1) methods and then forecasted drought duration by using the first-order and second-order MC models. They showed that the second-order MC models with DAR (1) forecasted drought duration at the monthly time scale better than the first-order of MC models with the empirical transition probability matrix. Based on Sharma & Panu (2012), it is highlighted that the self-dependency of the truncated drought index is not a negligible factor in forecasting drought duration.

Alternating renewal-reward (ARR) model. While MC and DARMA models have been used in forecasting drought duration, occurrence time, and interarrival time, realizing mutual correlation among duration, interarrival time, and severity alludes to the need for forecasting all drought characteristics simultaneously (Mishra *et al.* 2009). The ARR model is capable of forecasting occurrence time, duration, interarrival time, and severity simultaneously (Kendall & Dracup 1992; Mishra *et al.* 2009). The ARR model considers duration and severity as random variables and, in turn, fits durations and severities of the predefined frequent durations by geometric and gamma distributions, respectively (Kendall & Dracup 1992). Therefore, once a drought event starts with randomly sampled duration, D, from a geometric distribution, drought severity is estimated by aggregating D times randomly sampled drought index values from a gamma distribution. Kendall & Dracup (1992) showed that the one-step-ahead estimated mean, standard deviation, and autocorrelation coefficient from the ARR models are close to those of observations. In addition, the estimated frequency of severe drought events is not underestimated. However, the prominent issue with the ARR model is caused by the insufficient sub-sample number of durations and severities when those are fitted to probability distribution functions (Kendall & Dracup 1992). In this context, González & Valdés (2003) used historic and tree ring paleo reconstruction data in the ARR model.

The parameters of MC, DARMA, and ARR models are estimated, based on the observations of the truncated drought index values under the assumption of stationarity. Therefore, they may not successfully forecast drought characteristics under global warming.

Post-application of the theory of runs

Since some of stochastic models and most of the statistical, dynamical, and hybrid models handle continuous variables, drought duration, interarrival time, and severity can be inferred simultaneously by applying the theory of runs after a drought index is forecasted. Therefore, how accurately peaks, trend, and variability of a drought index are forecasted at different lead-times is important in this approach. In this context, we synthesize drought forecasting methods in four broad categories: stochastic, statistical, dynamical, and hybrid statistical-dynamical modeling.

Stochastic drought forecasting models

Conditional probability models. Conditional probability models forecast future values conditioned on self-correlated or/and cross-correlated variables (Hao *et al.* 2016c, 2018). The joint probability distribution, which is inherently associated with a conditional probability model, represents the relationship between predictors and predictand. Since conditional probability models can easily incorporate nonlinearly related variables into forecasting, these models have been widely used in a wide range of hydroclimate studies, including drought forecasting (Cancelliere *et al.* 2007; Maity & Nagesh Kumar 2008; Wong *et al.* 2009; Araghinejad 2011; Khedun *et al.* 2014; Hao *et al.* 2016c,

2018). Prediction using the conditional probability model is conceptually equal to the probability distribution of the forecasted value such that the conditional probability model provides the expectation and its variance (Cancelliere *et al.* 2007) (see mathematical expressions in Appendix 2D of supplement file-2). Therefore, it facilitates the quantification of uncertainty of prediction (Hao *et al.* 2016c).

For example, Hao *et al.* (2016c) forecasted Standardized Runoff Index (SRI) in Texas by using SRI and SPI in previous time steps as predictors in a conditional probability model. The forecast skill was compared with Ensemble Streamflow Prediction (ESP) as a baseline drought prediction. Although variable correlations between SRI and antecedent SPI caused seasonal and regional variation in forecasting skill, the overall performance of the conditional forecasting method outperformed ESP. However, its forecasting accuracy and reliability reduced as lead-time increased. Once SRI was forecasted, the probability of occurrence of drought, which had more severity than the moderate drought (e.g., −0.8), was calculated. They also showed that the estimated high probability of drought occurrence agreed well with the historical drought events in the case of a 1-month lead-time. However, conditional probability models, as any other data-driven forecasting models, explore serial dependence and cross-correlation based on only observed data. Therefore, to improve forecasting accuracy and reliability and reflect the nonstationarity of drought into the model, long historical observations of predictand and predictors are required.

To build the joint probability distribution, it is necessary that predictand and predictors have common marginal distributions. However, when incorporating a large number of predictors, this requirement is not always satisfied and establishing a dependence structure is difficult in high dimensions (Hao & Singh 2016; Hao *et al.* 2018). To compromise the issues in high dimensions, the vine copula method can be used due to its flexibility in handling dependence structures (Joe 1994; Hao & Singh 2016; Hao *et al.* 2018).

Copula models. The mutual dependence among drought characteristics requires multivariate analysis for drought risk analysis and drought forecasting (Mishra & Singh 2011; Zhang *et al.* 2013; Reddy & Singh 2014; Xiao *et al.* 2017). Since drought occurrence and propagation are related to the ocean-atmospheric teleconnection and initial hydrologic conditions, drought forecasting can be implemented by using joint distribution models (Hao *et al.* 2016c). AghaKouchak (2015) forecasted drought using the Multivariate Standardized Drought Index (MSDI) based on the joint distribution of precipitation and soil moisture (SM), and forecasting was done using ESP over East Africa. The forecasted MSDI with ESP showed that the accuracy of forecasts was acceptable up to a 4-month lead-time but was critically affected by initial conditions and climate of the target month. However, different hydroclimate variables may have marginal distributions belonging to different families such that the conventional joint distribution models may not successfully mimic the dependence structures (Mishra & Singh 2011; Khedun *et al.* 2014; Madadgar & Moradkhani 2014). Copula models, which build dependent relationships among d (the number of variables) variables using their copula function in the d-dimensional unit hypercube with the uniform distributions, are not limited to the type of marginal distributions (Grimaldi & Serinaldi 2006; Khedun *et al.* 2014; Zhang & Singh 2019). Therefore, copula models have been widely adopted to forecasting precipitation and streamflow (Lee & Salas 2011; Hao & Singh 2013; Khedun *et al.* 2014), besides their application to developing drought index and multivariate drought (e.g., severity-duration-areal) frequency analysis (Wong *et al.* 2009; Hao & AghaKouchak 2013; Yang *et al.* 2018; Zhang & Singh 2019).

Since copula models have various families, finding the optimal copula model and estimating parameters of copula functions are important. The procedure to fit marginal distribution functions and estimate the optimal parameters of copula functions can be found in Appendix 2D of supplement file-2.

Copula models have been used to forecast drought index and occurrence/transition of drought state in terms of temporal and spatial extent (Madadgar & Moradkhani 2013, 2014; Xiao *et al.* 2017; Dehghani *et al.* 2019). For example, Madadgar & Moradkhani (2013) forecasted one-season-ahead drought (spring streamflow conditioned on winter drought state) using 3-month aggregated streamflow fitted to the Gaussian copula for the Gunnison River basin of the upper Colorado River basin in the U.S. The forecasted streamflow outperformed ESP (as a benchmark method)

and observed streamflow fell inside an estimated 90% confidence interval. Based on the forecasted streamflow and confidence interval, they could forecast a drought state and its occurrence probability. Madadgar & Moradkhani (2013) was successfully extended to forecast seasonal drought and its occurrence probability in the spatial extent by Madadgar & Moradkhani (2014). Dehghani *et al.* (2019) probabilistically modeled the propagation of meteorological drought to hydrological drought or normal to wet conditions using the Clayton copula, which belongs to the Archimedean copula family, for Karun River basin in the southwest Iran.

Besides the forecasting of drought indicators/indices, copula models can also forecast the transition of drought state with its occurrence probability, so practitioners can decide whether drought will be getting more severe or terminate at a certain level of confidence in the next season and have benefit in managing water resources. Copula has also been widely used in drought analysis (e.g., Thilakarathne & Sridhar 2017; Montaseri *et al.* 2018; Ayantobo *et al.* 2019; Samantaray *et al.* 2019). For example, Thilakarathne & Sridhar (2017) analyzed drought risk in the Lower Mekong River basin by using the Gumbel-Hougaard copula for trivariate distributions of severity, duration, and peak which were driven from 3-month SPI. However, copula models also require the stationarity assumption for fitting marginal distributions and estimating parameters of copula functions. Therefore, copula models may not fully reflect nonstationarity embedded in drought signals or drought indicators.

Statistical drought forecasting models

Statistical forecasting methods utilize persistent and periodic characteristics of drought index and/or statistically significant covariation between drought index and drought indicators (Cordery & McCall 2000; Mishra & Singh 2011; Hao *et al.* 2018). However, to forecast drought in a skillful manner, finding predictors, which can explain a greater percentage of variability of predictand, is important (Cordery & McCall 2000). Since drought is attributed to multiple hydroclimate variables and various frequency bands of SST anomalies, a wide range of drought indicators with long enough observation periods are required. When multiple predictors have multicollinearity, authentic relationships between predictors and predictand are deluded by redundant predictors (Graham 2003). To avoid problems caused by multicollinearity, the PCA and canonical correlation analysis (CCA) can be used to reduce the dimensionality of multiple predictors (Hao *et al.* 2018). Since each statistical model has a distinct way to apply predictors to forecasting processes, we discuss the widely used statistical models, including time series models, regression models, and machine learning models.

Time series models. Time series models forecast future data values by linearly aggregating previously observed values based on weights for least squares estimation (Mishra & Desai 2005; Shumway & Stoffer 2017). Autoregressive Integrated Moving Average (ARIMA) is a representative time series model. While ARIMA is proposed for non-seasonal or non-periodic time series, the multiplicative seasonal ARIMA (SARIMA) can be used when the time series has seasonal cyclic patterns (Mishra & Desai 2005; Fernández *et al.* 2009). The mathematical theory of ARIMA and SARIMA can be found in Appendix 2D of supplement file-2.

ARIMA and SARIMA are the generalized versions of ARMA to forecast nonstationary time series (Mishra & Desai 2005; Hao *et al.* 2018). While regular differencing in ARIMA relaxes the drift term in time series, SARIMA has both regular and seasonal differencing terms to relax trend and seasonal cyclic patterns.

Moghimi *et al.* (2019) forecasted seasonal drought based on the 3-month RDI (RDI3) by using subsets of ARIMA models (e.g., autoregressive (AR), moving average (MA), and ARMA) for 16 synoptic stations in the south of Iran and showed the applicability of ARIMA models in forecasting droughts. Mishra & Desai (2005) forecasted SPI by using ARIMA and SARIMA in the Kanasabati River basin in India. They showed statistical similarities of mean and variance of observed and forecasted data at a 1-month lead-time. The coefficient of correlation (CC) reduced as a lead-time increase. Han *et al.* (2010) used ARIMA for forecasting the forthcoming 10-day period of Vegetation Temperature Condition Index (VTCI) for the Guanzhong Plain in the northwest of China. Since they used spatiotemporal data, ARIMA models were fitted at each pixel and, in turn, the spatial extent of forecasted VTCI and its error were easily estimated. Consequently, they showed 65.7% of forecasted data had a mean standard error between −0.1 and

0.1. Since ARIMA uses only the self-dependency nature of the drought index itself, it has limitations in considering the land-atmospheric feedback in drought occurrence and development. The importance of using explanatory variables was highlighted by Fernández *et al.* (2009). They forecasted Standardized Streamflow Index (SSFI) by using the ARIMA model incorporating Martonne index expressed as a ratio of precipitation to temperature as an explanatory variable to the predictand. As a result, the model showed an improved root mean square error (RMSE) when compared with the RMSE of the conventional ARIMA model. Besides, nonlinear relationships and time-dependent feedbacks between drought indicators, which are important to estimate drought occurrence, may be easily ignored in time series models (Hao *et al.* 2018; Fung *et al.* 2019). Machine learning models are appropriate to consider nonlinear relationships between predictors and predictand due to their inherent nonlinear nature (Fung *et al.* 2019).

Regression models. Various regression models have been used in a wide range of hydro-climatology and water management studies (Cordery & McCall 2000; Adamowski *et al.* 2012; Hao *et al.* 2016a, 2016b, 2018; to name a few). Multivariate regression models forecast unobserved values based on covariation between observed predictand and predictors and hypotheses of temporal and spatial dependency in predictand and predictors.

In forecasting drought index as a predictand, predictors may be any of the drought indicators, such as ENSO, PDO, precipitation, streamflow, and soil moisture, as long as they have a significant correlation with the predictand (Kumar & Panu 1997; Liu & Juárez 2001; Barros & Bowden 2008). For example, Liu & Juárez (2001) forecasted monthly Normalized Difference Vegetation Index (NDVI) from 1951 to 1998 for a 4-month lead-time in northwest Brazil using various ENSO indices, including Niño-3.4, Southern Oscillation Index (SOI), Dipole 2, North Atlantic Sea Surface Temperature (NATL), and South Atlantic Sea Surface Temperature (SATL). They showed that the model accurately forecasted seasonal drought and drought occurrence. Since forecasting NDVI efficiently displays the spatial extent of drought truncated below a specified threshold, it can replace drought indicators that suffer from spatial sparsity. Barros & Bowden (2008) forecasted 12-month SPI (SPI12) across the Murray-Darling basin, Australia, by using predictors, including SST anomalies across the Indian and Pacific oceans, a zonal gradient of outgoing longwave radiation (OLR) over the Pacific Ocean, and far western Pacific wind-stress anomalies. Although 12-month lead-time forecasting of the spatially averaged SPI12 showed a high level of accuracy, spatial errors were large in the area which had high regional variations of rainfall but had a low density of rainfall gauges. Besides, the uncertainty of forecasts increases when more redundant predictors are used in the model. Therefore, finding predictors, which increase fitness to observations and reduce uncertainty, is an important element in the multiple linear regression (MLR) model. When predictand values are an ordinal variable like drought categories of the U.S. Drought Monitor (USDM), Hao *et al.* (2016a, 2016b) used the ordinal regression (OR) model to forecast drought categories by using predictors, including 6-month SPI (SPI6), 3-month SRI (SRI3), and 3-month running mean of soil moisture percentile (SMP). Since OR uses the logit function, which links forecasted continuous variable by MRL to the non-exceedance probability of corresponding specified drought category, it allows one to forecast categorical observations (Hao *et al.* 2016a, 2016b, 2018).

Although ENSO related variables, such as SST anomalies, geopotential height, and SOI, are associated with drought occurrence and variability of precipitation, it may not have concurrent effects on the hydroclimate in inland areas but may show time lag effects on the predictand (Cordery & McCall 2000). Therefore, the linearity between predictors and predictand is less able to capture physical mechanisms such that long-term forecasting may not be successful (Mishra & Singh 2011; Hao *et al.* 2016c). A piecewise nonlinear regression model can be used to consider the nonlinear relationship between predictors and predictand, and forecast nonstationary drought index by partitioning the time series (Mohseni *et al.* 1998; Vanli & Kozat 2014).

Although piecewise nonlinear regression has been applied to forecast drought under global warming, partitioning is a subjective matter and the representative slope governing predictors-predictor relationship is not derived (Mohseni *et al.* 1998). In addition, to capture nonstationarity and periodicity of time series, long historical observations are required (Barros & Bowden 2008). As machine learning

models have gained attention due to their effective nonlinear representativeness, stand-alone machine learning models or machine learning (e.g., Self-Organizing Map (SOM)) coupled with multivariate regression models have been used to improve forecasting skill (Barros & Bowden 2008; Lin & Wu 2009). Therefore, the popularity of a stand-alone regression model for drought forecasting has been reduced (Fung *et al.* 2019).

Machine learning models. Nonlinear relationships and temporal dependencies (lag effects) between hydrologic variables have posed limitations on statistical models that have the hypothesis of linearity (Cordery & McCall 2000; Mishra & Singh 2011; Hao *et al.* 2018). However, machine learning models successfully find nonlinear patterns between predictors and predictand due to their learning capability stemming from their model structure and nonlinear functions in neurons (Mishra & Singh 2011; Belayneh & Adamowski 2012; Hao *et al.* 2018). Therefore, machine learning models, including Artificial Neural Networks (ANNs), Fuzzy-Logic (FL), and Support Vector Machines (SVMs), have been applied to various studies related with pattern classification and forecasting (Kim & Valdés 2003; Mishra & Desai 2006; Mishra *et al.* 2007; Bacanli *et al.* 2009; Belayneh & Adamowski 2012; Özger *et al.* 2012; Hao *et al.* 2018). Structures and traits of machine learning models (i.e., ANNs, FL, and SVMs) are discussed in Appendix 2D of supplement file-2.

To improve drought forecasting skills of machine learning models, wavelet transform is integrated into Fuzzy-Logic (Wavelet-FL), ANNs (Wavelet-ANNs) and SVMs (Wavelet-SVMs) (Kim & Valdés 2003; Özger *et al.* 2012; Belayneh *et al.* 2014; Deo *et al.* 2017b). The wavelet transform decomposes time series into each frequency band and eliminates noise, such that signals which have significant frequencies can be selectively used in drought forecasting. Kim & Valdés (2003) applied Wavelet-ANNs in forecasting PDSI for the Conchos River basin of northern Mexico. They showed that data preprocessing with wavelet transform improved the forecasting accuracy (RMSE and hit rates) for varying lead-time (from 1 to 12 months) compared with conventional ANNs. As one expects, however, the forecasting accuracy degrades as a lead-time increases. Özger *et al.* (2012) applied Wavelet-FL to forecasting the Palmer modified drought index (PMDI) and showed that Wavelet-FL forecasted acceptable accuracy with a coefficient of determination of 0.8 at a 12-month lead-time. Belayneh *et al.* (2014) applied ARIMA, ANN, support vector regression (SVR), Wavelet-ANNs, and Wavelet-SVMs for the forecasting of SPI in the Awash River basin in Ethiopia. They showed that the machine learning models outperformed the time series model and the preprocessing of data using wavelet transforms increased the forecasting accuracy compared with conventional machine learning models.

Dynamical drought forecasting models

Near-real-time drought forecasting or early warning has been implemented by using coupled general circulation models (CGCMs) which can enable future climate projections based on ocean-atmosphere-land physical processes (Delworth *et al.* 2002; Yuan & Wood 2013). To forecast climate and weather, CGCMs have been used by a wide array of climate forecast systems, such as National Centers for Environmental Prediction (NCEP) Climate Forecast System Version 2 (CFSv2), Canadian Coupled Climate Model Versions 3 and 4 (CanCM3, CanCM4), and European Center for Medium Range Weather Forecasting (ECMWF) seasonal forecast system 4 (SYS4) (Molteni *et al.* 2011; Yuan & Wood 2013; Saha *et al.* 2014). While statistical forecasting models forecast future climate or drought in the range of observed values and suffer from reflecting the nonstationary nature of climate systems, climate models based on CGCMs are relaxed from those limitations. However, climate models have systematic biases and coarse spatial resolutions and are largely influenced by initial conditions as well (Doblas-Reyes *et al.* 2013; Hao *et al.* 2018; Krinner & Flanner 2018). To forecast reliable agricultural and hydrological droughts, terrestrial water budgets with the least errors and fine resolutions should be estimated by hydrological models forced by climate models (Wanders & Wood 2016). Therefore, to improve the performance of dynamical drought forecasting models, climate models are required to be post-processed. We will discuss how climate models are post-processed for improving forecasting skills in Appendix 2E of supplement file-2. Then limitations of multimodel ensemble forecasts and dynamical forecasting

models coupling hydrologic models with climate models are discussed in the following subsections.

Multimodel ensemble forecast. Increases in the understanding of climate systems and additional observations (e.g., remote sensing measurements) enable better forecasting from climate models. However, their forecasts of temperature and precipitation for extratropical areas are not satisfactory due to the unrevealed chaotic nature of complex ocean-atmospheric circulation systems (Kumar *et al.* 2013; Yuan & Wood 2013). Furthermore, climate forecasts from an individual climate model are sensitive to initial conditions of oceanic or atmospheric state (Doblas-Reyes *et al.* 2013). Beyond the bias correction and downscaling methods mentioned in Appendix 2E of supplement file-2, the inter-model integration approach, which is referred to as the multimodel ensemble, has been adopted to improve sub-seasonal to annual climate forecasting (Palmer *et al.* 2004; Kirtman *et al.* 2014; Wanders & Wood 2016).

Multimodel ensemble models aim to compensate for errors of individual climate models and quantify uncertainties by merging multiple climate models with different initial conditions. North American Multimodel Ensemble (NMME) (Kirtman *et al.* 2014) and the Development of a European Multimodel Ensemble System for Seasonal-to-Interannual Prediction (DEMETER) system (Palmer *et al.* 2004) are representative multimodel ensemble forecasting systems. To improve multimodel ensemble forecasting, besides simple ensemble mean, weighted ensemble mean using step-wise regression or multiple regression, and Bayesian Modeling Averaging (BMA) have been applied (Krishnamurti *et al.* 1999; Ma *et al.* 2016; Wanders & Wood 2016). Whereas different ensemble weighing methods result in different degrees of gain in climate forecasting skills, it can be generalized that multimodel ensemble models outperform any other single climate model. Besides, multimodel ensemble models show statistically significant forecasting skills for 1 to 2 months of lead-time (Mo & Lyon 2015). However, a challenge that remains in multimodel ensemble is to increase its forecasting skill. Lorenz *et al.* (2018) explained the low forecasting skills of the Climate Forecasting System (CFS) of NMME by pointing out a significant increase in the accuracy of drought forecasts when replacing the forecasted CFS with observed variables when the probability of USDM intensification is forecasted.

Multimodel ensemble models enhance the forecasting of drought onset and enable probabilistic drought forecasts compared to single climate models. However, it was also found that an increase in the hit rate (increase in detectability) accompanied an increase in the false alarm rate (decrease in reliability) (Yuan & Wood 2013). Turco *et al.* (2017) evaluated the forecast accuracy and reliability of ECMWF SYS4 for drought (SPEI6) in August from 1981 to 2010 across Europe. The ECMW SYS4 forecasted the spatial patterns of SPEI6 and drought occurrence conditions (e.g., from extreme to normal) close to the observations up to a 2-month lead-time. Although the CC reduces as a lead-time increases, it showed greater than 0.6 of median up to a 2-month lead-time. Besides, the probability of forecast of drought occurrences, which are less than −0.8 of SPEI, was less than the observed one. The hit rate, in general, is greater than the false alarm rate but an increase in the false alarm rate along with an increase in the hit rate is detected as well. Forecasting skills of dynamical models are strongly affected by the strength of ENSO teleconnection and climate models are likely to over-represent the SST-drought relationship (Cohen & Jones 2011; Yuan & Wood 2013). Therefore, the asymmetric behavior between detectability and reliability might be caused by internal atmospheric variability and less nonlinear SST-drought relationship in climate models (Yuan & Wood 2013; Mo & Lyon 2015). Furthermore, the global drought onset detectability by multimodel ensemble is ~30% on average (Yuan & Wood 2013). Therefore, 'whether seasonal forecasting of drought onset at regional scales is essentially a stochastic forecasting problem' is an open question (Yuan & Wood 2013).

Coupling hydrological models for drought forecasting. Soil moisture, streamflow, and groundwater level are important drought indicators for agricultural and hydrological drought forecasting (Hao *et al.* 2018). Based on the long memory span of drought indicators, the ESP method can be used for their forecasting. The ESP implements a hydrologic model by forcing it with randomly sampled atmospheric forcings (e.g., precipitation, temperature, and wind speed) (Day 1985; Shukla *et al.* 2013; Hao *et al.* 2018). However, the

forecasting skill of ESP generally loses its statistical significance after a 1-month lead-time. A fallback method then uses forecasts from climate models/multimodel ensemble method to drive hydrologic models or crop growth simulation models, including the Variable Infiltration Capacity (VIC) model, the Soil & Water Assessment Tool (SWAT), and the Community Land Model (CLM) (Mo & Lettenmaier 2014; Shafiee-Jood *et al.* 2014; Yuan *et al.* 2015; Infanti & Kirtman 2016). In a recent study, Sehgal *et al.* (2018) and Sehgal & Sridhar (2019) evaluated the accuracy of water budget and drought indices (percentile of surface and total soil moisture) which were forecasted by using SWAT with the input of NCEP CFSv2 for the South Atlantic-Gulf region in the U.S. Each forecasted water budget component (i.e., SM, runoff) and percentile of SM had high accuracy but caution was required, since the accuracy degraded after a 1-month lead-time (Sehgal *et al.* 2018; Sehgal & Sridhar 2019). Kang & Sridhar (2018) evaluated weekly drought forecasting using SWAT and VIC with CFSv2 as forcing. They found that forecast accuracy degraded after a 2-month lead-time due to an increase in uncertainty of CFSv2 and showed that overall MSDI has a better agreement with the USDM drought severity map than did univariate drought indices (e.g., Standardized Soil Moisture Index (SSI) and Standardized Baseflow Index (SBI)). Besides, to reflect more realistic surface-groundwater exchange into a land-surface model, Kang & Sridhar (2019) applied the VIC model integrated with the Modular Three-Dimensional Finite-Difference Ground-Water Flow model (MODFLOW) and assessed droughts using MSDI in the Chesapeake Bay watershed in the U.S. They showed that the integrated version of the VIC model improved the assessment of drought characteristics when compared to the original VIC model. This suggests that land-atmospheric models may have gaps to reflect more realistic physical phenomena for better drought forecasting.

The reliability of dynamical climate forecast (CF) influences the hydroclimate forecast from hydrological models. Besides that, the forecasting skill of a hydrological model is largely influenced by initial hydrological conditions (IHCs), such that their forecasting skill varies with when (season) and where (hydrological regime) forecasting is undergone (Maurer *et al.* 2004; Wood & Lettenmaier 2008; Shukla & Lettenmaier 2011; Mahanama *et al.* 2012; Hao *et al.* 2018). Ma *et al.* (2019) forecasted seasonal soil moisture drought using a distributed time-variant gain model (DTVGM) hydrologic model with bias-corrected and downscaled NMME as a forcing, which is referred to as NMME-DTVGM, in the upper Han River basin in China. They showed that the NMME-DTVGM was affected by IHCs and the forecast skill of NMME by explaining the regional and seasonal variation of accuracy in forecasts of intensity and detectability of soil moisture drought. Although IHCs generally include snowpack, antecedent soil moisture, groundwater, and water storage in reservoirs, a number of studies mainly focused on the roles of snow water equivalent (SWE) and SM in assessing the forecast skill of hydrological models (Li *et al.* 2009; Mahanama *et al.* 2012; Shukla *et al.* 2013; Hao *et al.* 2018). Wood & Lettenmaier (2008) found that the forecast skill is largely affected by IHCs (SWE and SM) during the transition period from wet to dry seasons. In contrast, CF mainly influenced the forecast skill during the transition period from dry to wet seasons. Mahanama *et al.* (2012) evaluated the effect of IHCs on streamflow forecast across the contiguous United States (CONUS) and observed that streamflow forecast was mainly influenced by SWE during snow melting seasons and SM exerted statistically significant effects on the skill during fall and winter seasons. Shukla & Lettenmaier (2011) assessed the effect of IHCs and CF on the seasonal forecasts of cumulative runoff (CR) and SM by using VIC models in different seasons at different lead times and across the CONUS. They found that IHCs dominated CR forecasts during winter and spring in the Souris-Red-Rainy, Upper Mississippi, and Great Lakes regions. In the western U.S. (Pacific Northwest, California, Great Basin, and Lower Colorado), during spring (MAM) and summer (mainly June) months, IHCs provided forecast skill for CR forecast up to the 6-month lead-time. In the eastern U.S. (New England, Mid-Atlantic, the northeast of South Atlantic-Gulf, and Ohio), IHCs affected the CR forecast at less than 2-month lead-time during winter and spring seasons. After the lead-time of which IHCs significantly affected CR forecast, CF started to influence the CR forecast. However, in Tennessee, Lower Mississippi, and the west of the South Atlantic-Gulf regions CR forecasts were dominated by CF at all lead times. IHCs generally dominated SM forecasts at a 1-month lead-time

across the CONUS. However, some regions in the midwest and western U.S. showed SM forecasts were influenced by IHCs up to the lead-time of 5 months when forecasting began in winter or spring seasons.

Understanding the effect of IHCs on the hydroclimate forecast is important, since it allows a forecaster to put weight on the decisive contributor (either IHCs or CF) such that improved forecast skill can be obtained. Furthermore, it is found that forecast initialized in the summer season with dry IHCs is mainly affected by IHCs. Besides, the level of impact of IHCs in the summer season significantly varies at different lead times. It suggests that properties or signals of IHCs largely affect hydroclimate forecasts during drought events (Shukla *et al.* 2013).

Hybrid statistical-dynamical forecasting models

Rationales and limitations of statistical and dynamical forecasting methods were explained in the previous sections of stochastic, statistical, and dynamical drought forecasting models. The prominent limitations of statistical methods are due to the nonlinear relationship between drought indicators and SST teleconnections and the nonstationary nature of climate systems (Mishra & Singh 2011; Fung *et al.* 2019). In contrast, dynamical models lack long-term forecastability and stochastic nature of ocean-atmosphere circulation and show high variability of forecasting skill in space and time, in sequence, leading to low forecast skill of hydrological models (Madadgar *et al.* 2016). For better drought forecasting, it is important to make optimal use of complementary relationships between statistical and dynamical models (Madadgar *et al.* 2016; Hao *et al.* 2018).

Hybrid statistical-dynamical forecasting modeling framework is to merge forecasts from statistical and dynamical models (Madadgar *et al.* 2016; Hao *et al.* 2018). Since the conveyance of uncertainty of forecasts benefits the decision-making process, regression methods, Bayesian posterior distribution, and BMA have been widely used as merging methods to facilitate probabilistic forecasts (Schepen *et al.* 2014; Schepen & Wang 2015; Hao *et al.* 2018; Strazzo *et al.* 2019). The Bayes theorem-based merging methods have gained attention, since they reduce the uncertainty of forecast and improve out-of-sample forecastability (Xu *et al.* 2018).

Hybrid statistical-dynamical models have shown better forecasting skills than either statistical or dynamical methods alone (Schepen *et al.* 2014; Schepen & Wang 2015; Madadgar *et al.* 2016; Xu *et al.* 2018; Strazzo *et al.* 2019). For example, Xu *et al.* (2018) forecasted SPI6 in China by using BMA to merge forecasts from statistical models (ESP, ANN, SVM, Wavelet-ANN, and Wavelet-SVM) and climate models (NMME). They showed that their hybrid model outperformed single statistical and dynamical models by enabling skillful long-term forecasting and reduced the false alarm rate of drought onset by 25% compared with dynamical models. Madadgar *et al.* (2016) applied the Expected Advice (EA) algorithm (Cheng & Aghakouchak 2015) to merge statistical (Bayesian copula functions) and dynamical (NMME) forecast models to forecast precipitation anomalies and infer the degree of wetness and dryness in the southwestern U.S. They evaluated the accuracy of forecasts using the level of correspondence to the spatial extent of the observed negative anomalies of precipitation and showed that the developed hybrid model outperformed both single models and the improved forecasting skills up to ~50% compared to the dynamical model, especially in extremely dry years from 2014 to 2015. Forecasting skills of dynamical models and hybrid models are affected by how significant the dependence structure between ocean-atmosphere-land and local hydroclimate variables and reliable model parameterization are established. Therefore, long historic and spatially dense observations are important for reliable drought forecasting.

Attempts to improve hybrid statistical-dynamical model performance have been made by exploring new merging techniques that can best complement statistical and dynamical models. In this context, a Bayesian post-processing technique, the so-called calibration, bridging, and merging (CBaM) method (Schepen *et al.* 2014; Schepen & Wang 2015), was developed, which successfully enhanced climate forecasting of multimodel ensemble models in the hybrid statistical-dynamical modeling framework (Schepen *et al.* 2014; Schepen & Wang 2015; Strazzo *et al.* 2019). The calibration module is a statistical model that establishes a relationship between dynamical forecasts and observations to correct dynamical model forecasts. The bridging module is similar to the calibration component but relates the dynamical model and the SST anomaly teleconnection, such as

ENSO, PDO and, IOD, to overcome the failure of dynamical models in representing the SST teleconnection and hydroclimate variability. The merging module combines forecasts from the calibration and bridge modules by using BMA. Therefore, the improved forecasting skill of hybrid statistical-dynamical model provides more reliable forcing variables for better drought forecasting. Therefore, it is also an important research area to explore optimal merging methods of integrating statistical and dynamical models.

DROUGHT AND TREE MORTALITY

Drought does not only directly alter atmosphere and terrestrial water budgets via the water cycle system connected by precipitation and evapotranspiration, but also has impacts on productivity and survival of forest which affect carbon cycles and climate (Pan & Wood 2006; McDowell *et al.* 2008; van Mantgem *et al.* 2009; Allen *et al.* 2010; Williams *et al.* 2013). Terrestrial ecosystems regulate land-surface albedo, net radiation, evapotranspiration, and soil moisture such that regional and global climates are characterized by it (Sud *et al.* 1990; Bonan *et al.* 1992). A representative example is Amazonian deforestation and its impacts on the regional increase in surface temperature and decrease in precipitation, evapotranspiration, and runoff (Nobre *et al.* 1991; Bonan *et al.* 1992; Gash & Nobre 1997). As global mean temperature increases and severe large-scale droughts are accompanied, water scarcity and high temperature predispose trees/forests to die-off (McDowell *et al.* 2008; Allen *et al.* 2010; Williams *et al.* 2013). Therefore, to prevent large-scale tree mortality and reduce its detrimental feedback on climate, understanding the mechanisms of tree mortality influenced by drought is important.

Causative mechanisms of tree mortality

Hydraulic failure

When transpiration (E) occurs through leaves, the water loss is compensated for by absorbing water from soil and transporting water through the xylem to the leaves, where water diffuses into the atmosphere. The movement of water in the xylem is driven by the difference in the water potentials between the rhizosphere and leaf (Sperry *et al.* 1998, 2002; McDowell *et al.* 2008). A mathematical expression of E is expressed as:

$$E = K(\psi_s - \psi_l - \rho_w g h) \quad (1)$$

where K is the hydraulic conductance specified by leaf of a plant; ψ_s and ψ_l are the soil water potential and leaf water potential, respectively; ρ_w is the density of water; g is the gravitational acceleration; and h is the height of the stem.

The increase in temperature and dry atmospheric conditions raise atmospheric water demand. However, under dry conditions, limited water supply from the rhizosphere causes the vapor-pressure deficit (VPD): a more greatly reduced soil water potential (ψ_s) leads to higher VPD (McDowell *et al.* 2008; Williams *et al.* 2013; Klein 2014). The increase of E reduces the leaf water potential (ψ_l) as long as the hydraulic conductance specified by the leaf of a plant (K) remains constant (Figure 2) (Sperry *et al.* 1998; McDowell *et al.* 2008). However, after surpassing a certain point of ψ_l, air intrudes into the xylem through pit pores, in sequence, the cavitation and embolization of xylem initiate. When the xylem is 100% embolized, K becomes zero and its corresponding E and ψ_l are called E_{crit} and ψ_{crit}, respectively (Sperry *et al.* 1998; McDowell *et al.* 2008). When ψ_l exceeds ψ_{crit}, hydraulic failure occurs such

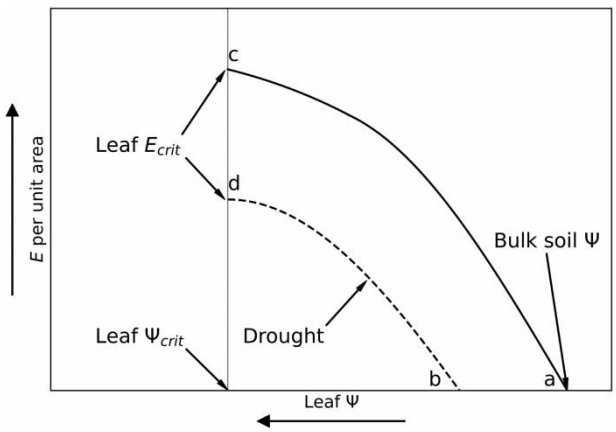

Figure 2 | Evapotranspiration per unit leaf area as a function of leaf water potential (ψ_l) when soil moisture is plenty (solid curve) and when soil moisture is reduced by drought condition (dashed line) (McDowell *et al.* 2008).

that trees die. Since, under drought conditions, ψ_s is lowered and trees have a small margin of safety to ψ_{crit} (dashed line in Figure 2), trees are prone to die-off (Sperry *et al.* 1998; McDowell *et al.* 2008). Therefore, when drought intensity/severity is high, hydraulic failure is likely to bring up tree die-off (McDowell *et al.* 2008). However, the vulnerability to hydraulic failure varies with the xylem structure of species, biomes and edaphic characteristics (e.g. soil texture, structure, and porosity) (McDowell *et al.* 2008; Klein 2014).

Carbon starvation

To avoid hydraulic failure, trees regulate E not to reach E_{crit} by controlling stomatal conductance (G_s). Trees have distinct patterns in regulating E or ψ_l, and the patterns categorize the trees into isohydric and anisohydric species (Sperry *et al.* 1998, 2002; McDowell *et al.* 2008; Allen *et al.* 2010; Klein 2014; Roman *et al.* 2015; Hochberg *et al.* 2018). Isohydric species maintain relatively constant ψ_l regardless of ψ_s (McDowell *et al.* 2008; Breshears *et al.* 2009; Klein 2014; Roman *et al.* 2015; Hochberg *et al.* 2018). Some examples of isohydric trees are black walnut, populus balsamifera, prunus simonii, and piñon (McDowell *et al.* 2008; West *et al.* 2008; Attia *et al.* 2015; Roman *et al.* 2015). Anisohydric species modulate ψ_l as a function of ψ_s and maintain an overall higher G_s than isohydric species do (McDowell *et al.* 2008; Klein 2014). Anisohydric species are exemplified by juniper, eucalyptus, sunflower, sugar maple, and populus balsamifera (McDowell *et al.* 2008; Attia *et al.* 2015; Roman *et al.* 2015).

Isohydric species close stomata not to drop ψ_l below the midday leaf water potential when ψ_s decreases. In contrast, anisohydric species continue transpiration as long as extractable water remains. The early shutdown of stomatal conductance leads to the ceasing of photosynthesis and carbon uptakes, such that reserved carbohydrates are used for maintaining metabolism, root production, and respiration. Therefore, isohydric species are predisposed to mortality mainly due to carbon starvation. On the other hand, anisohydric species tend to elongate the carbon assimilation process up to far negative ψ_l, which is likely to cause cavitation in the xylem. As a consequence, anisohydric species are predisposed to mortality due to hydraulic failure. In this context, one can induce the effect of drought duration and intensity on the mortality of trees as follows: (1) severe drought leads to steep decreasing slope of ψ_s and die-off of anisohydric species due to hydraulic failure in the early stage of drought; (2) longer persistent drought leads to shallow decreasing slope of ψ_s and leads to the mortality of isohydric species due to carbon starvation and die-off of anisohydric species follows.

Threats of biotic agent

Trees, which suffer or have been suffering from drought, are susceptible to the threats of biotic agents (e.g., insects and pathogens) due to embolized xylem and reduced ability to maintain homeostasis (McDowell *et al.* 2008; McDowell 2011). To protect trees from biotic agents, trees produce defensive bio-chemicals, such as resin (McDowell *et al.* 2008; Allen *et al.* 2010). However, carbon starving during or after drought lowers productivity in producing the defensive materials but increases the production of volatile compounds, such as ethanol, which attract biotic agents (McDowell *et al.* 2008; Allen *et al.* 2010; McDowell 2011). Biotic agents accelerate the occlusion of xylem by injecting fungi inside trees and facilitate the depletion of reserved carbohydrates, since trees have to produce more defensive chemical compounds and allocate them (McDowell *et al.* 2008; Allen *et al.* 2010).

Furthermore, drought, which accompanies high temperatures, increases growing seasons of biotic agents and, in turn, amplifies the population of biotic agents (McDowell *et al.* 2008). When carbon starved trees have synchronous periods of high population of biotic agents, tree mortality increases. Besides the effect of biotic agents, wildfires have caused tree mortality by combustion and damaging tissues of trees (McDowell *et al.* 2008; Williams *et al.* 2010). The expected rise of global temperature increases the population of biotic agents and occurrences of wildfires which contribute to tree mortality. Although hydraulic failure, carbon starvation, and attack of biotic agents are primary mechanisms of tree mortality during drought, tree mortality is also influenced by dominant species, age, and recovery function after damage (Keane *et al.* 2001; Choat *et al.* 2018). Therefore, forecasting tree mortality is a complex task with high uncertainty. We will discuss the forecastability of tree mortality in the following.

Dynamic vegetation models to forecast tree mortality

To forecast drought-driven tree mortality, it is necessary to understand tree mortality mechanisms at an individual tree and extend the understanding to probabilistic mortality risk factors at large scales (Hartmann *et al.* 2018). Even though tree mortality causative mechanisms are elucidated, survival and succumbing to drought depend on xylem structure, root distribution, age, and stand density of trees (Hickler *et al.* 2012; Brodribb *et al.* 2019). Since tree mortality is affected by species of trees and competition with other trees, incorporating biomass diversity and individual tree physiology into tree mortality forecasting models is important (Aubry-Kientz *et al.* 2019). Many dynamic vegetation models (DVMs), such as Lund-Potsdam-Jena (LPJ), General Ecosystem Simulator (referred to as GUESS), SILVA, ForClim, and LANDIS-II, have been used to forecast tree mortality (Scheller & Mladenoff 2004; Mette *et al.* 2009; Bircher *et al.* 2015; Bugmann *et al.* 2019). DVMs can be categorized into three modeling frameworks following theoretical models, empirical models, and mechanistic (hydraulic) models (Bugmann *et al.* 2019).

Theoretical models

Theoretical models, which are based on mathematical formulae rather than empirical relationships, include the self-thinning rule, and process-based models which characterize the functioning of stages of phenology (Yoda 1963; Li *et al.* 2000; Hickler *et al.* 2012; Hülsmann *et al.* 2018). The self-thinning rule relates the average tree biomass to stand density using a power-law described as:

$$\overline{BM} = \zeta \rho^{\gamma} \tag{2}$$

where $\overline{BM}$ is the average biomass; ρ is the stand density; and ζ and γ are the thinning coefficients where $-3/2$ is conventionally taken for γ.

The self-thinning rule is a macroscopic approach such that it lacks specific causal mechanisms of how individual trees respond and acclimate to the spatial arrangement of community (Li *et al.* 2000). Other representative methods in this category are process-based models represented by 'forest gap models,' including ForClim, JABOWA (named after last names of authors: Janick, Botkin and Wallis), GUESS, Ecosystem Demography model (ED), and LPJ dynamical global dynamical vegetation model (Botkin *et al.* 1972; Bugmann 1996; Smith *et al.* 2001; Hickler *et al.* 2012; McDowell *et al.* 2016; Bugmann *et al.* 2019).

Process-based models, which are based on carbon balance between assimilation and allocation (or deduction) for growth and maintaining homeostasis, are implemented on independent patches which are characterized by plant functional types (PFT) (Smith *et al.* 2001; Fischer *et al.* 2016; Bugmann *et al.* 2019). PFT implicitly represents allometric responses (growth and physiology related with biomass) and primary production under limited soil water and light, and allows one to group trees based on similar type, such as height of matured tree, crown structure (e.g., length, diameter and projection area) and shade tolerance (Smith *et al.* 2001; Fischer *et al.* 2016). On each patch, processes of tree phenology, which are compartmented with tree growth, regeneration, competition, and mortality, are estimated at a time step of a year by specified equations for each process as a function of PFT-specific coefficients, soil water content, temperature, leaf area index (LAI) and light (Fischer *et al.* 2016). Chaste *et al.* (2019) applied LPJ-LMfire in the boreal forests of Canada to estimate the potential change in dominant biomass (e.g., Abies, Picea, Pinus, and Populus) under global warming scenarios. The LPJ-LMfire is an extended model of LPJ to incorporate wildfire emissions, intensity, spread, and fire-driven tree mortality. They showed the reduction of biomass and the change of taxa (from conifer to broadleaf trees) in the southern boreal regions under the Representative Concentration Pathway (RCP) 8.5 scenario. ForClim models have been widely used in forecasting structures and functioning of forests due to their reliability in estimating forest dynamics (e.g., Bugmann 1996; Bircher *et al.* 2015; García-Valdés *et al.* 2018; Huber *et al.* 2018; Thrippleton *et al.* 2019). Since process-based models have a large number of parameters, knowing influential processes and parameters is beneficial for model calibration and model development. However, Huber *et al.* (2018) showed that process-based models were not dominated by a single process and parameter and described that the sensitivity of influential parameters varied following species, assemblages of species, phenology, and site-specific

properties. Therefore, identifying the sensitive parameters in all states of systems of interest will improve the applicability of the model for a wide range of species and states of systems (Huber *et al.* 2018). To forecast drought-driven tree mortality with least uncertainty, modeling at regional scales integrated with both empirical and forest inventory data is required (McDowell *et al.* 2016; Vanoni *et al.* 2019). McDowell *et al.* (2016) applied ED, which is a process-based regional-scale model (Moorcroft *et al.* 2001), to forecast the mortality of needle-leaf trees in the southwest U.S. by 2100. When McDowell *et al.* (2016) compared the likelihood of mortality of needle-leaf evergreen trees (*Pinus edulis* and *Juniperus monosperma*) obtained from the empirical correlative model, ED, and dynamic global vegetation models (DGVMs), all models consistently forecasted extensive loss of the conifer trees, while DGVMs underestimated the tree mortality. The underestimation of DGVMs stemmed from their lack of some process modules that accounted for outbreaks of insects/pathogens, rising frequency of wildfire, and failure of a succession of trees (McDowell *et al.* 2016). Although process-based models can take climate change into consideration (Reyer *et al.* 2014), individual tree mortality is defined when a random number drawn from Poisson process random sampling with an expectation of PFT-based reproduction rate of a patch at the previous year is below a background threshold. Therefore, they could not consider individual physiology and hydraulic failure mechanisms which are critical in drought conditions (Smith *et al.* 2001).

Empirical models

Empirical models forecast tree mortality, based on a statistically driven growth-mortality relationship (Cailleret *et al.* 2017; Bugmann *et al.* 2019). Empirical models base their hypotheses accordingly (Bigler & Bugmann 2004; Cailleret *et al.* 2016, 2017; Hülsmann *et al.* 2018): tree ring-width data can represent individual physiology, including productivity and carbon availability; rates of radial stem growth are affected by available water, temperature, and abiotic factors; most dying trees show reduced growth rates before dieback. On the other hand, the robustness of the hypothesis of models is degraded by sampling errors and variability of survival strategy of species to stress factors (Cailleret *et al.* 2017). For example, dry-tolerant species live longer even when growth rates are decreased and unspecified height for cutting to measure tree size also adds to uncertainties. Besides, windthrow, wildfire, outbreak of biotic agents, and flooding (waterlogging) predispose trees to die-off suddenly irrespective of tree growth (Hülsmann *et al.* 2018). Despite those concerns, empirical models have been widely used to forecast tree mortality as a pragmatic alternative to process-based models (Adams *et al.* 2013; Hülsmann *et al.* 2018). Empirical models relate mortality status (survival = 0 or dieback = 1) to ring-width (diameter measurement at breast height (DBH)) using logistic regression (Cailleret *et al.* 2016; Hülsmann *et al.* 2018) as:

$$p_{i,\Delta t=1} = logit^{-1}(X_i\theta) = \frac{e^{(X_i\theta)}}{1+e^{(X_i\theta)}} \tag{3}$$

where $p_{i,\Delta t=1}$ represents the probability of mortality at a 1-month lead-time for tree i; X_i are the predictors; and θ denotes the parameters.

The annual probability of mortality can be projected to a mortality period of Δt years as:

$$p_{i,\Delta t} = 1 - (1 - p_{i,\Delta t})^{\Delta t} \tag{4}$$

Then, $p_{i,\Delta t}$ is fitted to the observed mortality status to estimate parameter θ. Hülsmann *et al.* (2018) incorporated mean annual precipitation and temperature into predictors to improve forecasting skill.

However, most of the theoretical and empirical models fail to represent observed regional patterns of forest, since they ignore biomass diversity and individual tree physiology, and lack of mechanistic representation (i.e., hydraulic failure) (Aubry-Kientz *et al.* 2019; Bugmann *et al.* 2019). Furthermore, they are inaccurate in forecasting the timing of tree die-off (Bigler & Bugmann 2004). Process-based and empirical models have relative differences to each other such that complementary relationships can be established (Adams *et al.* 2013). While process-based models depict processes of tree development as causal phenological feedbacks to environmental stress, empirical models rely on a correlative relationship between mortality and biomass (Smith *et al.* 2001; Cailleret *et al.* 2016; Fischer *et al.* 2016;

Hülsmann *et al.* 2018). Therefore, process-based models represent more comprehensive causal mechanisms using multiple compartmentalized processes, whereas they have higher uncertainties due to many associated parameters (Adams *et al.* 2013; Fischer *et al.* 2016). In contrast, empirical models have relatively smaller uncertainty but they are likely to result in severe bias when extrapolation is beyond the observed range of variability (Adams *et al.* 2013). To utilize the advantages of both models, empirical models and process-based models can be merged. For example, Hülsmann *et al.* (2018) used an empirical model in the process of mortality calculation in the process-bases model (ForClim) and improved the forecast skill. Thrippleton *et al.* (2019) evaluated the impacts of merging empirical models (e.g., growth-based and competition-based models) with ForClim and showed the importance of merging a proper empirical model when forecasting forest dynamics at regional scales by comparing the accuracy in forecasts of ForClim merged with different empirical models in Europe: the growth-based models brought more consistent improvement in ForClim than using competition-based models which lack variables directly affected by the harsh environment.

The prominent limitation in the field of dynamic forecasting tree mortality is that mechanistic causal algorithms, which explain hydraulic failure and its association with carbon starvation, are not fully incorporated in forecasting models due to the difficulty in demonstrating mortality caused by hydraulic failure in nature (Adams *et al.* 2013; Bugmann *et al.* 2019). To forecast tree mortality under drought conditions, incorporating the mechanistic causal algorithms is important, and it enables one to forecast when, where, and how trees will die (Brodribb *et al.* 2019).

Mechanistic (hydraulic) models

Mechanistic models simulate tree mortality based on the interaction between soil water availability and stomatal regulation to secure water in trees (Martin-StPaul *et al.* 2017; Brodribb *et al.* 2019). Since mechanistic or hydraulic models utilize the vulnerability of xylem (how much safety margin trees have) of each species against water stress conditions, they allow one to track dysfunctions of hydraulic systems of trees and forecast time of tree dieback (Brodribb *et al.* 2019). As shown in Figure 2, the safety of margin is decreased as soil water contents reduce. However, different species have different safety margins, and differently coordinate stomatal closure once embolism is initiated. Besides, trees acclimate to change in the environment such that trees are likely to have more drought-tolerance and greater safety of margin (Martin-StPaul *et al.* 2017; Larter *et al.* 2017). Therefore, for the sake of successful hydraulic modeling, thorough data meta-analysis should be done for each species in different climates (Martin-StPaul *et al.* 2017). Data meta-analysis implies processes as follows: monitoring cavitation of xylem by excision, x-ray tomography or optical devices (Figure 3(a)); establishing relationship of loss of hydraulic conductivity (or cumulative volumes of embolisms) as a function of available water in trees (ψ_l) (Figure 3(b)); finding threshold of cumulative volumes of embolism which lead trees dieback (Cochard *et al.* 2015; Choat *et al.* 2016; Martin-StPaul *et al.* 2017; Brodribb *et al.* 2019). For example, 50% of embolism triggers die-off of conifer and angiosperms are predisposed to death after 88% of embolism (Brodribb *et al.* 2019).

Hydraulic flow models have been used to estimate forest mortality under contemporary drought conditions, not future conditions (Sperry *et al.* 1998; Anderegg *et al.* 2015). For forecasting purposes, SurEau was developed to imply future variation of available soil water reserve in mechanistic models (Martin-StPaul *et al.* 2017; Brodribb *et al.* 2019; Cochard 2019). SurEau establishes an empirical relationship between the percent of loss of plant hydraulic conductance (PLC) and water reserved in trees by fitting the collected embolism data to a sigmoid function as:

$$\mathrm{PLC} = \frac{1}{1 + \exp\left[(\alpha/25)(\psi_l - \psi_{eb})\right]} \tag{5}$$

where α is a shape parameter of sigmoid function; ψ_l means water potential of xylem or leaf; ψ_{eb} denotes water potential causing embolism corresponding to embolism resistance. For example, ψ_{eb} of angiosperms is the magnitude of water potential causing 88% embolism.

The estimated PLC at a certain ψ_l is used in the calculation of hydraulic conductance of leaf (K), water release from apoplast pathway (cavitation; W_{ap}) and symplast pathway (W_{sy}). Then, soil water reserve (WR) is estimated by summing up previous WR values and a balance between E

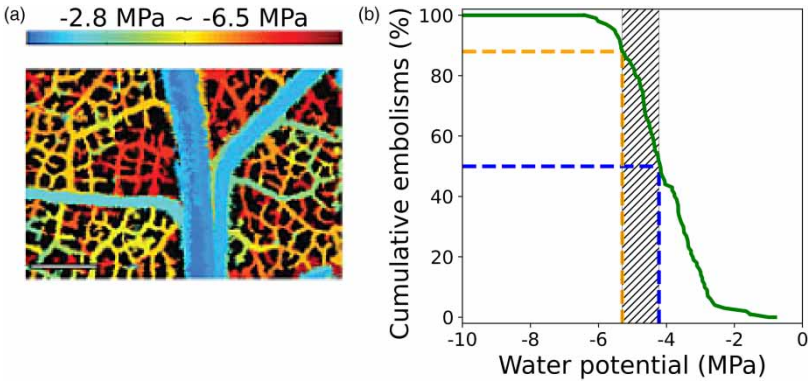

Figure 3 | (a) Optically observed leaf water potential where xylem cavitation occurs (colored location), (b) cumulative embolisms against water potential in trees (green curve). Blue (orange) dashed line represents water potential corresponding to 50% (88%) of embolism. Gray hatched area represents a range of tree mortality likely to occur in case of *Quercus robur* plant (Brodribb *et al.* 2019). Please refer to the online version of this paper to see this figure in color: http://dx.doi.org/10.2166/wcc.2020.239.

and W_{ap} and W_{sy} as:

$$WR_{t+1} = WR_t - E + W_{ap} + W_{sy} \tag{6}$$

where E is the transpiration calculated by:

$$E = E_{\max} \times f(\psi_l) \times LA \tag{7}$$

where $E_{\max}$ is the maximum rate of transpiration; $f(\psi_l)$ is stomatal regulation function (slope of the linear part of a sigmoid function); and LA is a plant leaf area.

The estimated WR is used as extractable soil water to calculate ψ_s. Finally, the estimated ψ_s, K, and E are used in Equation (1) for which in turn a new ψ_l is calculated for the next time step. Therefore, the time of tree die-off can be forecasted by finding the instance where 100% of embolism occurs. It is confirmed that mechanistic models estimate ψ_l and ψ_s which are regulated by the xylem cavitation. For more details on calculational processes, reference is made to Martin-StPaul *et al.* (2017). Brodribb *et al.* (2019) used SurEau to forecast mortality of *Fagus sylvatica* forest in central France by 2100 and showed tree mortality would abruptly increase after 2020 with an accompanying reduction in genetic diversity. Cochard (2019) elucidated that trees reached the time of tree die-off earlier when heatwaves occurred together with drought by showing impacts of temperature on VPD, hydraulic conductance of leaf (K), and leaf cuticular conductance through simulation using SurEau. The interesting finding of Cochard (2019) is that an occurrence of heatwaves after drought onset (already under water-stress condition) leads to tree die-off significantly earlier than the case of simultaneous onset of heatwaves and drought. Mechanistic models require the knowledge of physiology about individual species and extensive data collection. However, once reliable data inventory is established, this framework for tree mortality modeling is efficient to forecast which species will die under drought conditions.

SOIL DEGRADATION AND TREE DIE-OFF

Besides direct impacts of drought on tree mortality, soil degradation and waterlogging (flooding and/or irrigation) can cause tree die-off. Natural climate variability like drought and anthropogenic activities on agriculture and ecosystems accelerate desertification which represents land degradation (Dregne & Chou 1992). Reduced vegetation covers and soil compaction contribute to land degradation by facilitating wind erosion of fine soil grains and organic minerals from surface soil and diminishing water infiltration and water holding capacity of the soil (Belnap 1995; Castellano & Valone 2007; D'Odorico *et al.* 2013). Although the aforementioned desertification contributors bring out a hostile rhizosphere against plant growth, salinization exerts drought-like hydraulic failure on plants (Munns 2002; D'Odorico *et al.* 2013; Kath *et al.* 2015).

Salinization can be caused by over-irrigation or waterlogging which derive higher water table and accumulation of salinity in the root zone of soil (Dregne & Chou 1992; Thomas & Middleton 1993). However, in dry conditions,

removal of vegetation (increased seepage), lowered groundwater level, and remobilization of soluble salinity from soil profile to near-surface through capillary exfiltration cause salinization (Munns 2002; D'Odorico *et al.* 2013; Kath *et al.* 2015). Saline soil reduces water potential in the rhizosphere and retards water uptake by trees (D'Odorico *et al.* 2013; Kath *et al.* 2015). In the early stage of exposure to saline soil, trees suffer from reduced water uptake due to osmotic effects. However, as the intrusion of salt increases in plant tissues, the density of salinity in a plant rises to a toxic level such that cell processes stop carbon assimilation and growth (Munns 2002; D'Odorico *et al.* 2013).

Kath *et al.* (2015) investigated the impacts of salinity and changes in groundwater level on buffering effects of groundwater to the die-off of riverine forests. They concluded that when riverine forests were connected to shallow groundwater systems during drought, tree mortality increased due to salinization, rather than buffering trees from dieback.

Trees which survive after going through drought may not have enough vascular functions and metabolisms to efficiently maintain homeostasis and fend outer stress. Therefore, in poorly managed irrigation over lands, drought termination may increase the level of salinization and predispose the weakened trees to die-off rather than prospering trees.

FUTURE PROSPECTS

Countless endeavors to improve the accuracy in forecasts have developed various drought and tree mortality forecasting methods. However, most of the drought and tree mortality forecasting models have room to advance one step further. This study makes a list of elements to improve forecasting skills for drought and tree mortality under global warming.

Forecasting of droughts

Perspective of modeling

Most statistical drought forecasting models, including stochastic models, show acceptable forecasting skills at lead times of less than 6 months. Machine learning models merged with wavelet extend lead-time up to 12 months. Forecasting skill of dynamical models degrades after a lead-time of 1 month. Under global warming, long-term drought forecasting with quantified uncertainties will help decision/policy makers establish a long-term drought mitigation plan. Entropy spectral analysis shows eligibility for long-term forecasting through application to various research areas, including geology, hydrology, and meteorology (Singh 1997, 2011; Cui & Singh 2016). Entropy spectral analysis does not impose any assumptions on unknown time series, while it identifies significant spectra with a high degree of resolution and minimizes bias of estimates (Krstanovic & Singh 1991a, 1991b). Entropy spectral analysis integrates stochastic model development and spectral analysis such that it is expected to forecast drought index, which is composed of periodic and stochastic components (Padmanabhan & Rao 1988). However, entropy spectral analysis was developed under the stationary assumption. Therefore, entropy-based forecasting methods, which can reflect second-order nonstationarity, will contribute to improving long-term drought forecasting either by themselves or merging with dynamical models. While forecasting drought index (hazard) has a long history of research, forecasting drought impact has gained attention only recently and it provides pragmatic drought preparedness information to policy makers and stakeholders (Sutanto *et al.* 2019). Drought impact forecasting can be implemented based on the established statistical relationship (drought impact function) between drought indices and drought impact data (Bachmair *et al.* 2015; Sutanto *et al.* 2019). Drought impact forecasting has usually been implemented for regions and categorized groups of impact. For robust drought impact forecasting, the completeness and long period of drought impact database (e.g., European Drought Impact report Inventory (EDII) for Germany and Drought Impact Reporter (DIP) for the U.S.) are the most important (Sutanto *et al.* 2019).

Perspective of data

The framework for drought forecasting modeling is primarily based on the SST teleconnection to regional climate variables. Since the SST teleconnection varies at interannual-to-multidecadal periods, records from only instrumental gauge networks cannot reveal patterns in decadal-to-multidecadal

periods. To characterize the variability of hydroclimate, which manifests a strong persistence of either wet or dry periods, at least 100–200 years of data are required (Thyer *et al.* 2006). Paleoclimate reconstruction compensates for the limitation of a short period of instrumental records. Cook *et al.* (2010) developed a paleoclimatic reconstruction of modified PDSI across the CONUS known as Living Blended Drought Atlas (LBDA). However, its uncertainties are highly variable at temporal and spatial scales due to the variation of acquisition of tree-ring data (Ho *et al.* 2018). Therefore, developing accurate paleoclimatic drought index maps can improve the understanding of hydroclimatic patterns with SST teleconnection.

To improve hydrological forecasting associated with dynamical models, meteorological forcing data need high reliability. However, tropical areas and developing countries in particular have sparse instrumental gauge networks, and even the density of the global meteorological gauge network has reduced in recent decades. Remote sensing data can be used in the areas which have gauge sparsity in order to improve hydroclimate monitoring. Furthermore, to better understand the hydraulic traits of the physiology of trees at regional or global scales, soil moisture and tree health monitoring with spatiotemporally fine resolutions are essential. Therefore, airborne equipped with a hyperspectral sensing tool will supplement in-situ observations, such as x-ray tomography and optical observation (Brodribb *et al.* 2019). However, since remotely sensed data has a systematic bias, reducing errors in the data by merging in-situ data is another research area.

Forecasting of tree mortality

Forecasting tree mortality has been done over areas colonized with the same species since common PFT facilitates parameterizing in DVMs. Since drought is likely to be more severe and have a larger areal extent under global warming, forecasting tree mortality at larger scales is necessary to understand drought implications on tree mortality in the future. Although process-based models (i.e., dynamic global vegetation models (DGVMs)) have been used for forecasting at continental-scale, their parameterization was done for too-coarse scales by using only widely distributed major species (Hickler *et al.* 2012). Therefore, DGVMs are not suitable to represent the regional-scale variation of tree mortality. Furthermore, since tree mortality is primarily attributed to hydraulic failure under drought conditions, mechanistic models may provide more accurate forecasts. Further studies to extend the application of mechanistic models to larger scales will improve forecasting tree mortality under global warming. Besides, a spatiotemporally extensive data-meta analysis should be done by using various monitoring measures (in-situ and remote sensing) to improve mechanistic forecasting models.

CONCLUSIONS

This study has reviewed forecasting methods for drought and tree mortality. Causative mechanisms of drought and tree mortality have been discussed, and implications of global warming for those causative mechanisms have also been elucidated.

Under global warming, temperature-driven hydrological processes and multiple hydrologic variables in drought assessment have been emphasized. Then, multivariate drought indices (e.g., self-calibrated Palmer Drought Severity Index (PDSI) with Penman-Monteith (pm) (sc_PDSI_pm)) which avoid the overestimation of potential evaporation (PE) and facilitate regional comparison have been developed. However, one needs to bear in mind that methods of PE calculation, quality of hydro-meteorological data, and selection of base period make a significant difference in drought assessment even when using the same drought index.

For statistical drought forecasting, models are required to be free from the stationarity of modeling frameworks such that they can consider the nonlinearity and nonstationarity nature of teleconnection and evolution of drought under global warming. Once long enough period observations that can convey a nonstationarity pattern are prepared, machine learning methods combined with wavelet transform and coupla-conditional probability methods are expected to provide acceptable forecasting skills.

Although dynamic drought forecasting models, based on general circulation models (GCMs) and multimodel ensemble models, inherently embed nonlinearity and nonstationarity, a linear correlation between SST anomalies and drought is likely to be over-represented in the dynamic models and overlook stochastic processes in the models. Therefore, to improve drought forecasts, hybrid

statistical-dynamic forecasting models were developed. Although their integrative processes improve probabilistic forecasting, those do not provide a standard rule for blending the benefits from statistical and dynamic models.

Severe and long-lasting droughts increase tree mortality due to hydraulic failure, carbon starvation, and threats of biotic agents. Whereas process-based and empirical tree mortality forecast models lack the effects of hydraulic failure that are the most important mechanisms under drought conditions, mechanistic (hydraulic) tree mortality models consider xylem cavitation and regulation of stomatal closure following the dynamic soil water reserve. Although mechanistic models require extensive data collection to establish embolism-water content relationships, they are expected to forecast tree mortality in drought conditions best. Tree die-off can last for an extended period after termination of drought due to the salinization of soil caused by the lowered groundwater level and inadequate irrigation.

Reliable forecasts of drought and tree mortality are essential for establishing drought mitigation plans and understanding environmental effects from ecosystems that are susceptible to climate change. Establishing densely populated observational networks, data assimilation with remote sensing data, and paleoclimatic reconstruction data help the practitioner to assess, monitor, and forecast drought and tree mortality with higher accuracy. Long-term drought forecasting (e.g., greater than 12 months of lead-time) and tree mortality forecasting at regional scales by using mechanistic models benefit monitoring and forecasting drought and drought-driven ecological degradation. Furthermore, U.S. Drought Monitor (USDM) is a good representation of improved drought early warning systems by cohesively coordinating drought research from multilevel governances (e.g., tribal, local, state, and federal partnerships). Like this, further improvement of forecasting drought and tree mortality can be accomplished by an intergovernmental and global collaboration of scientists and policymakers.

SUPPLEMENTARY MATERIAL

The Supplementary Material for this paper is available online at https://dx.doi.org/10.2166/wcc.2020.239.

REFERENCES

Adamowski, J., Fung Chan, H., Prasher, S. O., Ozga-Zielinski, B. & Sliusarieva, A. 2012 Comparison of multiple linear and nonlinear regression, autoregressive integrated moving average, artificial neural network, and wavelet artificial neural network methods for urban water demand forecasting in Montreal, Canada. *Water Resources Research* **48** (1). doi:10.1029/2010WR009945.

Adams, H. D., Williams, A. P., Xu, C., Rauscher, S. A., Jiang, X. & McDowell, N. G. 2013 Empirical and process-based approaches to climate-induced forest mortality models. *Frontiers in Plant Science* **4**, 438. doi:10.3389/fpls.2013.00438.

AghaKouchak, A. 2015 A multivariate approach for persistence-based drought prediction: application to the 2010–2011 East Africa drought. *Journal of Hydrology* **526**, 127–135. doi:10.1016/j.jhydrol.2014.09.063.

Akhtari, R., Morid, S., Mahdian, M. H. & Smakhtin, V. 2009 Assessment of areal interpolation methods for spatial analysis of SPI and EDI drought indices. *International Journal of Climatology: A Journal of the Royal Meteorological Society* **29** (1), 135–145. doi:10.1002/joc.1691.

Allen, C. D., Macalady, A. K., Chenchouni, H., Bachelet, D., McDowell, N., Vennetier, M., Kitzberger, T., Rigling, A., Breshears, D. D., Hogg, E. T. & Gonzalez, P. 2010 A global overview of drought and heat-induced tree mortality reveals emerging climate change risks for forests. *Forest Ecology and Management* **259** (4), 660–684. doi:10.1016/j.foreco.2009.09.001.

Anderegg, W. R., Flint, A., Huang, C. Y., Flint, L., Berry, J. A., Davis, F. W., Sperry, J. S. & Field, C. B. 2015 Tree mortality predicted from drought-induced vascular damage. *Nature Geoscience* **8** (5), 367. doi:10.1038/ngeo2400.

Anderegg, W. R., Martinez-Vilalta, J., Cailleret, M., Camarero, J. J., Ewers, B. E., Galbraith, D. & Powell, T. L. 2016 When a tree dies in the forest: scaling climate-driven tree mortality to ecosystem water and carbon fluxes. *Ecosystems* **19** (6), 1133–1147. doi:10.1007/s10021-016-9982-1.

Araghinejad, S. 2011 An approach for probabilistic hydrological drought forecasting. *Water Resources Management* **25** (1), 191–200. doi:10.1007/s11269-010-9694-9.

Attia, Z., Domec, J. C., Oren, R., Way, D. A. & Moshelion, M. 2015 Growth and physiological responses of isohydric and anisohydric poplars to drought. *Journal of Experimental Botany* **66** (14), 4373–4381. doi:10.1093/jxb/erv195.

Aubry-Kientz, M., Rossi, V., Cornu, G., Wagner, F. & Hérault, B. 2019 Temperature rising would slow down tropical forest dynamic in the Guiana Shield. *Scientific Reports* **9** (1), 10235. doi:10.1038/s41598-019-46597-8.

Avilés, A., Célleri, R., Paredes, J. & Solera, A. 2015 Evaluation of Markov chain based drought forecasts in an Andean regulated river basin using the skill scores RPS and GMSS. *Water Resources Management* **29** (6), 1949–1963. doi:10.1007/s11269-015-0921-2.

Ayantobo, O. O., Li, Y. & Song, S. 2019 Multivariate drought frequency analysis using four-variate symmetric and asymmetric Archimedean copula functions. *Water Resources Management* **33** (1), 103–127. doi:10.1007/s11269-018-2090-6.

Bacanli, U. G., Firat, M. & Dikbas, F. 2009 Adaptive neuro-fuzzy inference system for drought forecasting. *Stochastic Environmental Research and Risk Assessment* **23** (8), 1143–1154. doi:10.1007/s00477-008-0288-5.

Bachmair, S., Kohn, I. & Stahl, K. 2015 Exploring the link between drought indicators and impacts. *Natural Hazards and Earth System Sciences* **15** (6), 1381–1397. doi:10.5194/nhess-15-1381-2015.

Barros, A. P. & Bowden, G. J. 2008 Toward long-lead operational forecasts of drought: an experimental study in the Murray-Darling river basin. *Journal of Hydrology* **357** (3–4), 349–367. doi:10.1016/j.jhydrol.2008.05.026.

Beguería, S., Vicente-Serrano, S. M. & Angulo-Martínez, M. 2010 A multiscalar global drought dataset: the SPEIbase: a new gridded product for the analysis of drought variability and impacts. *Bulletin of the American Meteorological Society* **91** (10), 1351–1356. doi:10.1175/2010BAMS2988.1.

Belayneh, A. & Adamowski, J. 2012 Standard precipitation index drought forecasting using neural networks, wavelet neural networks, and support vector regression. *Applied Computational Intelligence and Soft Computing* **2012**, 1–13. doi:10.1155/2012/794061.

Belayneh, A., Adamowski, J., Khalil, B. & Ozga-Zielinski, B. 2014 Long-term SPI drought forecasting in the Awash River Basin in Ethiopia using wavelet neural network and wavelet support vector regression models. *Journal of Hydrology* **508**, 418–429. doi:10.1016/j.jhydrol.2013.10.052.

Belnap, J. 1995 Surface disturbances: their role in accelerating desertification. *Environmental Monitoring and Assessment* **37** (1–3), 39–57. doi:10.1007/BF00546879.

Berg, A. & Sheffield, J. 2018 Climate change and drought: the soil moisture perspective. *Current Climate Change Reports* **4** (2), 180–191. doi:10.1007/s40641-018-0095-0.

Bigler, C. & Bugmann, H. 2004 Predicting the time of tree death using dendrochronological data. *Ecological Applications* **14** (3), 902–914. doi.org/10.1890/03-5011.

Bigler, C., Bräker, O. U., Bugmann, H., Dobbertin, M. & Rigling, A. 2006 Drought as an inciting mortality factor in Scots pine stands of the Valais, Switzerland. *Ecosystems* **9** (3), 330–343. doi:10.1007/s10021-005-0126-2.

Bircher, N., Cailleret, M. & Bugmann, H. 2015 The agony of choice: different empirical mortality models lead to sharply different future forest dynamics. *Ecological Applications* **25** (5), 1303–1318. doi:10.1890/14-1462.1.

Bonan, G. B., Pollard, D. & Thompson, S. L. 1992 Effects of boreal forest vegetation on global climate. *Nature* **359** (6397), 716–718. doi:10.1038/359716a0.

Botkin, D. B., Janak, J. F. & Wallis, J. R. 1972 Some ecological consequences of a computer model of forest growth. *The Journal of Ecology* 849–872. doi:10.2307/2258570.

Breshears, D. D., Myers, O. B., Meyer, C. W., Barnes, F. J., Zou, C. B., Allen, C. D., McDowell, N. G. & Pockman, W. T. 2009 Tree die-off in response to global change-type drought: mortality insights from a decade of plant water potential measurements. *Frontiers in Ecology and the Environment* **7** (4), 185–189. doi:10.1890/080016.

Brodribb, T. J., Cochard, H. & Dominguez, C. R. 2019 Measuring the pulse of trees; using the vascular system to predict tree mortality in the 21st century. *Conservation Physiology* **7** (1), coz046. doi:10.1093/conphys/coz046.

Bugmann, H. K. 1996 A simplified forest model to study species composition along climate gradients. *Ecology* **77** (7), 2055–2074. doi:10.2307/2265700.

Bugmann, H. K., Seidl, R., Hartig, F., Bohn, F., Brůna, J., Cailleret, M., François, L., Heinke, J., Henrot, A. J., Hickler, T. & Hülsmann, L. 2019 Tree mortality submodels drive simulated long-term forest dynamics: assessing 15 models from the stand to global scale. *Ecosphere* **10** (2), e02616. doi:10.1002/ecs2.2616.

Cai, W., Santoso, A., Wang, G., Yeh, S. W., An, S. I., Cobb, K. M., Collins, M., Guilyardi, E., Jin, F. F., Kug, J. S. & Lengaigne, M. 2015 ENSO and greenhouse warming. *Nature Climate Change* **5** (9), 849–859. doi:10.1038/nclimate2743.

Cailleret, M., Bigler, C., Bugmann, H., Camarero, J. J., Cufar, K., Davi, H., Mészáros, I., Minunno, F., Peltoniemi, M., Robert, E. M. & Suarez, M. L. 2016 Towards a common methodology for developing logistic tree mortality models based on ring-width data. *Ecological Applications* **26** (6), 1827–1841. doi:10.1890/15-1402.1.

Cailleret, M., Jansen, S., Robert, E. M., Desoto, L., Aakala, T., Antos, J. A., Beikircher, B., Bigler, C., Bugmann, H., Caccianiga, M. & Čada, V. 2017 A synthesis of radial growth patterns preceding tree mortality. *Global Change Biology* **23** (4), 1675–1690. doi:10.1111/gcb.13535.

Cancelliere, A. & Salas, J. D. 2010 Drought probabilities and return period for annual streamflows series. *Journal of Hydrology* **391** (1–2), 77–89. doi:10.1016/j.jhydrol.2010.07.008.

Cancelliere, A., Di Mauro, G., Bonaccorso, B. & Rossi, G. 2007 Drought forecasting using the standardized precipitation index. *Water Resources Management* **21** (5), 801–819. doi:10.1007/s11269-006-9062-y.

Castellano, M. J. & Valone, T. J. 2007 Livestock, soil compaction and water infiltration rate: evaluating a potential desertification recovery mechanism. *Journal of Arid Environments* **71** (1), 97–108. doi:10.1016/j.jaridenv.2007.03.009.

Chaste, E., Girardin, M. P., Kaplan, J. O., Bergeron, Y. & Hély, C. 2019 Increases in heat-induced tree mortality could drive reductions of biomass resources in Canada's managed boreal forest. *Landscape Ecology* **34** (2), 403–426. doi:10.1007/s10980-019-00780-4.

Cheng, L. & AghaKouchak, A. 2015 A methodology for deriving ensemble response from multimodel simulations. *Journal of Hydrology* **522**, 49–57. doi:10.1016/j.jhydrol.2014.12.025.

Choat, B., Badel, E., Burlett, R., Delzon, S., Cochard, H. & Jansen, S. 2016 Noninvasive measurement of vulnerability to drought-induced embolism by X-ray microtomography. *Plant Physiology* **170** (1), 273–282. doi:10.1104/pp.15.00732.

Choat, B., Brodribb, T. J., Brodersen, C. R., Duursma, R. A., Lopez, R. & Medlyn, B. E. 2018 Triggers of tree mortality under drought. *Nature* **558** (7711), 531–539. doi:10.1038/s41586-018-0240-x.

Chung, C. H. & Salas, J. D. 2000 Drought occurrence probabilities and risks of dependent hydrologic processes. *Journal of Hydrologic Engineering* **5** (3), 259–268. doi:10.1061/(ASCE)1084-0699(2000)5:3(259).

Ciais, P., Reichstein, M., Viovy, N., Granier, A., Ogée, J., Allard, V., Aubinet, M., Buchmann, N., Bernhofer, C., Carrara, A. & Chevallier, F. 2005 Europe-wide reduction in primary productivity caused by the heat and drought in 2003. *Nature* **437** (7058), 529–533. doi:10.1038/nature03972.

Cochard, H. 2019 A new mechanism for tree mortality due to drought and heatwaves. *bioRxiv* 531632. doi:10.1101/531632.

Cochard, H., Delzon, S. & Badel, E. 2015 X-ray microtomography (micro-CT): a reference technology for high-resolution quantification of xylem embolism in trees. *Plant, Cell & Environment* **38** (1), 201–206. doi:10.1111/pce.12391.

Cohen, J. & Jones, J. 2011 A new index for more accurate winter predictions. *Geophysical Research Letters* **38** (21). doi:10.1029/2011GL049626.

Cook, B. I., Miller, R. L. & Seager, R. 2009 Amplification of the North American 'Dust Bowl' drought through human-induced land degradation. *Proceedings of the National Academy of Sciences* **106** (13), 4997–5001. doi:10.1073/pnas.0810200106.

Cook, E. R., Seager, R., Heim Jr, R. R., Vose, R. S., Herweijer, C. & Woodhouse, C. 2010 Megadroughts in North America: placing IPCC projections of hydroclimatic change in a long-term palaeoclimate context. *Journal of Quaternary Science* **25** (1), 48–61. doi:10.1002/jqs.1303.

Cook, B. I., Seager, R., Miller, R. L. & Mason, J. A. 2013 Intensification of North American megadroughts through surface and dust aerosol forcing. *Journal of Climate* **26** (13), 4414–4430. doi:10.1175/JCLI-D-12-00022.1.

Cook, B. I., Smerdon, J. E., Seager, R. & Cook, E. R. 2014 Pan-continental droughts in North America over the last millennium. *Journal of Climate* **27** (1), 383–397. doi:10.1175/JCLI-D-13-00100.1.

Cordery, I. & McCall, M. 2000 A model for forecasting drought from teleconnections. *Water Resources Research* **36** (3), 763–768. doi:10.1029/1999WR900318.

Cui, H. & Singh, V. P. 2016 Maximum entropy spectral analysis for streamflow forecasting. *Physica A: Statistical Mechanics and its Applications* **442**, 91–99. doi:10.1016/j.physa.2015.08.060.

Dai, A. 2011a Characteristics and trends in various forms of the Palmer Drought Severity Index during 1900–2008. *Journal of Geophysical Research: Atmospheres* **116** (D12). doi:10.1029/2010JD015541.

Dai, A. 2011b Drought under global warming: a review. *Wiley Interdisciplinary Reviews: Climate Change* **2** (1), 45–65. doi:10.1002/wcc.81.

Day, G. N. 1985 Extended streamflow forecasting using NWSRFS. *Journal of Water Resources Planning and Management* **111** (2), 157–170. doi:10.1061/(ASCE)0733-9496(1985)111:2(157).

Dehghani, M., Saghafian, B. & Zargar, M. 2019 Probabilistic hydrological drought index forecasting based on meteorological drought index using Archimedean copulas. *Hydrology Research* **50** (5), 1230–1250. doi:10.2166/nh.2019.051.

Delworth, T. L., Stouffer, R., Dixon, K., Spelman, M., Knutson, T., Broccoli, A., Kushner, P. & Wetherald, R. 2002 Review of simulations of climate variability and change with the GFDL R30 coupled climate model. *Climate Dynamics* **19** (7), 555–574. doi:10.1007/s00382-002-0249-5.

Deo, R. C., Tiwari, M. K., Adamowski, J. F. & Quilty, J. M. 2017b Forecasting effective drought index using a wavelet extreme learning machine (W-ELM) model. *Stochastic Environmental Research and Risk Assessment* **31** (5), 1211–1240. doi:10.1007/s00477-016-1265-z.

Doblas-Reyes, F. J., Andreu-Burillo, I., Chikamoto, Y., García-Serrano, J., Guemas, V., Kimoto, M., Mochizuki, T., Rodrigues, L. R. L. & Van Oldenborgh, G. J. 2013 Initialized near-term regional climate change prediction. *Nature Communications* **4**, 1715. doi:10.1038/ncomms2704. (2013).

D'Odorico, P., Laio, F. & Ridolfi, L. 2010 Does globalization of water reduce societal resilience to drought? *Geophysical Research Letters* **37** (13). doi:10.1029/2010GL043167.

D'Odorico, P., Bhattachan, A., Davis, K. F., Ravi, S. & Runyan, C. W. 2013 Global desertification: drivers and feedbacks. *Advances in Water Resources* **51**, 326–344. doi:10.1016/j.advwatres.2012.01.013.

Dong, B. & Sutton, R. T. 2007 Enhancement of ENSO variability by a weakened Atlantic thermohaline circulation in a coupled GCM. *Journal of Climate* **20** (19), 4920–4939. doi:10.1175/JCLI4284.1.

Dong, B., Sutton, R. T. & Scaife, A. A. 2006 Multidecadal modulation of El Nino–Southern Oscillation (ENSO) variance by Atlantic Ocean sea surface temperatures. *Geophysical Research Letters* **33** (8). doi:10.1029/2006GL025766.

Donohoe, A. & Battisti, D. S. 2011 Atmospheric and surface contributions to planetary albedo. *Journal of Climate* **24** (16), 4402–4418. doi:10.1175/2011JCLI3946.1.

Dregne, H. E. & Chou, N. T. 1992 Global desertification dimensions and costs. In: *Degradation and restoration of arid lands* (H. E. Dregne, ed). Texas Tech. University, Lubbock, pp. 249–282.

Enfield, D. B., Mestas-Nuñez, A. M. & Trimble, P. J. 2001 The Atlantic multidecadal oscillation and its relation to rainfall and river flows in the continental US. *Geophysical Research Letters* **28** (10), 2077–2080. doi:10.1029/2000GL012745.

FEMA. 1995 *National Mitigation Strategy: Partnership for Building Safer Communities*. Federal Emergency Management Agency, Washington, DC.

Fernández, C., Vega, J. A., Fonturbel, T. & Jiménez, E. 2009 Streamflow drought time series forecasting: a case study in a

small watershed in North West Spain. *Stochastic Environmental Research and Risk Assessment* **23** (8), 1063–1070. doi:10.1007/s00477-008-0277-8.

Fischer, R., Bohn, F., de Paula, M. D., Dislich, C., Groeneveld, J., Gutiérrez, A. G., Kazmierczak, M., Knapp, N., Lehmann, S., Paulick, S. & Pütz, S. 2016 Lessons learned from applying a forest gap model to understand ecosystem and carbon dynamics of complex tropical forests. *Ecological Modelling* **326**, 124–133. doi:10.1016/j.ecolmodel.2015.11.018.

Fu, Q. & Feng, S. 2014 Responses of terrestrial aridity to global warming. *Journal of Geophysical Research: Atmospheres* **119** (13), 7863–7875. doi:10.1002/2014JD021608.

Fu, X., Svoboda, M., Tang, Z., Dai, Z. & Wu, J. 2013 An overview of US state drought plans: crisis or risk management? *Natural Hazards* **69** (3), 1607–1627. doi:10.1007/s11069-013-0766-z.

Fung, K. F., Huang, Y. F., Koo, C. H. & Soh, Y. W. 2019 Drought forecasting: a review of modelling approaches 2007–2017. *Journal of Water and Climate Change* In press. doi:10.2166/wcc.2019.236.

García-Valdés, R., Bugmann, H. & Morin, X. 2018 Climate change-driven extinctions of tree species affect forest functioning more than random extinctions. *Diversity and Distributions* **24** (7), 906–918. doi:10.1111/ddi.12744.

Gash, J. H. C. & Nobre, C. A. 1997 Climatic effects of Amazonian deforestation: some results from ABRACOS. *Bulletin of the American Meteorological Society* **78** (5), 823–830. doi:10.1175/1520-0477(1997)078<0823:CEOADS>2.0.CO;2.

González, J. & Valdés, J. B. 2003 Bivariate drought recurrence analysis using tree ring reconstructions. *Journal of Hydrologic Engineering* **8** (5), 247–258. doi:10.1061/(ASCE)1084-0699(2003)8:5(247).

Graham, M. H. 2003 Confronting multicollinearity in ecological multiple regression. *Ecology* **84** (11), 2809–2815. doi:10.1890/02-3114.

Grimaldi, S. & Serinaldi, F. 2006 Asymmetric copula in multivariate flood frequency analysis. *Advances in Water Resources* **29** (8), 1155–1167. doi:10.1016/j.advwatres.2005.09.005.

Han, P., Wang, P. X., Zhang, S. Y. & Zhu, D. H. 2010 Drought forecasting based on the remote sensing data using ARIMA models. *Mathematical and Computer Modelling* **51** (11–12), 1398–1403. doi:10.1016/j.mcm.2009.10.031.

Hao, Z. & AghaKouchak, A. 2013 Multivariate standardized drought index: a parametric multi-index model. *Advances in Water Resources* **57**, 12–18. doi:10.1016/j.advwatres.2013.03.009.

Hao, Z. & Singh, V. P. 2013 Modeling multisite streamflow dependence with maximum entropy copula. *Water Resources Research* **49** (10), 7139–7143. doi:10.1002/wrcr.20523.

Hao, Z. & Singh, V. P. 2015 Drought characterization from a multivariate perspective: a review. *Journal of Hydrology* **527**, 668–678. doi:10.1016/j.jhydrol.2015.05.031.

Hao, Z. & Singh, V. P. 2016 Review of dependence modeling in hydrology and water resources. *Progress in Physical Geography* **40** (4), 549–578. doi:10.1177/0309133316632460.

Hao, Z., Hong, Y., Xia, Y., Singh, V. P., Hao, F. & Cheng, H. 2016a Probabilistic drought characterization in the categorical form using ordinal regression. *Journal of Hydrology* **535**, 331–339. doi:10.1016/j.jhydrol.2016.01.074.

Hao, Z., Hao, F., Xia, Y., Singh, V. P., Hong, Y., Shen, X. & Ouyang, W. 2016b A statistical method for categorical drought prediction based on NLDAS-2. *Journal of Applied Meteorology and Climatology* **55** (4), 1049–1061. doi:10.1175/JAMC-D-15-0200.1.

Hao, Z., Hao, F., Singh, V. P., Sun, A. Y. & Xia, Y. 2016c Probabilistic prediction of hydrologic drought using a conditional probability approach based on the meta-Gaussian model. *Journal of Hydrology* **542**, 772–780. doi:10.1016/j.jhydrol.2016.09.048.

Hao, Z., Singh, V. P. & Xia, Y. 2018 Seasonal drought prediction: advances, challenges, and future prospects. *Reviews of Geophysics* **56** (1), 108–141. doi:10.1002/2016RG000549.

Hartmann, H., Moura, C. F., Anderegg, W. R., Ruehr, N. K., Salmon, Y., Allen, C. D., Arndt, S. K., Breshears, D. D., Davi, H., Galbraith, D. & Ruthrof, K. X. 2018 Research frontiers for improving our understanding of drought-induced tree and forest mortality. *New Phytologist* **218** (1), 15–28. doi:10.1111/nph.15048.

Harzallah, A. & Sadourny, R. 1995 Internal versus SST-forced atmospheric variability as simulated by an atmospheric general circulation model. *Journal of Climate* **8** (3), 474–495. doi:10.1175/1520-0442(1995)008<0474:IVSFAV>2.0.CO;2.

Heim Jr, R. R.. 2002 A review of twentieth-century drought indices used in the United States. *Bulletin of the American Meteorological Society* **83** (8), 1149–1166. doi:10.1175/1520-0477-83.8.1149.

Hickler, T., Vohland, K., Feehan, J., Miller, P. A., Smith, B., Costa, L., Giesecke, T., Fronzek, S., Carter, T. R., Cramer, W. & Kühn, I. 2012 Projecting the future distribution of European potential natural vegetation zones with a generalized, tree species-based dynamic vegetation model. *Global Ecology and Biogeography* **21** (1), 50–63. doi:10.1111/j.1466-8238.2010.00613.x.

Ho, M., Lall, U. & Cook, E. R. 2018 How wet and dry spells evolve across the conterminous United States based on 555 years of paleoclimate data. *Journal of Climate* **31** (16), 6633–6647. doi:10.1175/JCLI-D-18-0182.1.

Hochberg, U., Rockwell, F. E., Holbrook, N. M. & Cochard, H. 2018 Iso/anisohydry: a plant–environment interaction rather than a simple hydraulic trait. *Trends in Plant Science* **23** (2), 112–120. doi:10.1016/j.tplants.2017.11.002.

Hoerling, M., Quan, X. W. & Eischeid, J. 2009 Distinct causes for two principal US droughts of the 20th century. *Geophysical Research Letters* **36** (19). doi:10.1029/2009GL039860.

Hoerling, M., Eischeid, J., Kumar, A., Leung, R., Mariotti, A., Mo, K., Schubert, S. & Seager, R. 2014 Causes and predictability of the 2012 Great Plains drought. *Bulletin of the American Meteorological Society* **95** (2), 269–282. doi:10.1175/BAMS-D-13-00055.1.

Hoskins, B. J. & Ambrizzi, T. 1993 Rossby wave propagation on a realistic longitudinally varying flow. *Journal of the*

Atmospheric Sciences **50** (12), 1661–1671. doi:10.1175/1520-0469(1993)050<1661:RWPOAR>2.0.CO;2.

Huber, N., Bugmann, H. & Lafond, V. 2018 Global sensitivity analysis of a dynamic vegetation model: model sensitivity depends on successional time, climate and competitive interactions. *Ecological Modelling* **368**, 377–390. doi:10.1016/j.ecolmodel.2017.12.013.

Hülsmann, L., Bugmann, H., Cailleret, M. & Brang, P. 2018 How to kill a tree: empirical mortality models for 18 species and their performance in a dynamic forest model. *Ecological Applications* **28** (2), 522–540. doi:10.1002/eap.1668.

Infanti, J. M. & Kirtman, B. P. 2016 Prediction and predictability of land and atmosphere initialized CCSM4 climate forecasts over North America. *Journal of Geophysical Research: Atmospheres* **121** (21), 12690–12701. doi:10.1002/2016JD024932.

Jacobs, P. A. & Lewis, P. A. W. 1977 A mixed autoregressive-moving average exponential sequence and point process (EARMA 1, 1). *Advances in Applied Probability* **9** (1), 87–104. doi:10.2307/1425818.

Joe, H. 1994 Multivariate extreme-value distributions with applications to environmental data. *Canadian Journal of Statistics* **22** (1), 47–64. doi:10.2307/3315822.

Kam, J., Stowers, K. & Kim, S. 2019 Monitoring of drought awareness from google trends: a case study of the 2011–17 California drought. *Weather, Climate, and Society* **11** (2), 419–429. doi:10.1175/WCAS-D-18-0085.1.

Kang, H. & Sridhar, V. 2018 Improved drought prediction using near real-time climate forecasts and simulated hydrologic conditions. *Sustainability* **10** (6), 1799. doi:10.3390/su10061799.

Kang, H. & Sridhar, V. 2019 Drought assessment with a surface-groundwater coupled model in the Chesapeake Bay watershed. *Environmental Modelling & Software* **119**, 379–389. doi:10.1016/j.envsoft.2019.07.002.

Kath, J., Powell, S., Reardon-Smith, K., El Sawah, S., Jakeman, A. J., Croke, B. F. & Dyer, F. J. 2015 Groundwater salinization intensifies drought impacts in forests and reduces refuge capacity. *Journal of Applied Ecology* **52** (5), 1116–1125. doi:10.1111/1365-2664.12495.

Kavvas, M. L. & Anderson, M. L. 1996 Extreme droughts. In: *Hydrology of Disasters*. (V. P. Singh, ed). Springer, Dordrecht, pp. 127–160.

Keane, R. E., Austin, M., Field, C., Huth, A., Lexer, M. J., Peters, D., Solomon, A. & Wyckoff, P. 2001 Tree mortality in gap models: application to climate change. *Climatic Change* **51** (3–4), 509–540. doi:10.1023/A:1012539409854.

Kendall, D. R. & Dracup, J. A. 1992 On the generation of drought events using an alternating renewal-reward model. *Stochastic Hydrology and Hydraulics* **6** (1), 55–68. doi:10.1007/BF01581675.

Khedun, C. P., Mishra, A. K., Singh, V. P. & Giardino, J. R. 2014 A copula-based precipitation forecasting model: investigating the interdecadal modulation of ENSO's impacts on monthly precipitation. *Water Resources Research* **50** (1), 580–600. doi:10.1002/2013WR013763.

Kim, T. W. & Valdés, J. B. 2003 Nonlinear model for drought forecasting based on a conjunction of wavelet transforms and neural networks. *Journal of Hydrologic Engineering* **8** (6), 319–328. doi:10.1061/(ASCE)1084-0699(2003)8:6(319).

Kirtman, B. P., Min, D., Infanti, J. M., Kinter III, J. L., Paolino, D. A., Zhang, Q., Van Den Dool, H., Saha, S., Mendez, M. P., Becker, E. & Peng, P. 2014 The North American multimodel ensemble: phase-1 seasonal-to-interannual prediction; phase-2 toward developing intraseasonal prediction. *Bulletin of the American Meteorological Society* **95** (4), 585–601. doi:10.1175/BAMS-D-12-00050.1.

Klein, T. 2014 The variability of stomatal sensitivity to leaf water potential across tree species indicates a continuum between isohydric and anisohydric behaviours. *Functional Ecology* **28** (6), 1313–1320. doi:10.1111/1365-2435.12289.

Krinner, G. & Flanner, M. G. 2018 Striking stationarity of large-scale climate model bias patterns under strong climate change. *Proceedings of the National Academy of Sciences* **115** (38), 9462–9466. doi:10.1073/pnas.1807912115.

Krishnamurti, T. N., Kishtawal, C. M., LaRow, T. E., Bachiochi, D. R., Zhang, Z., Williford, C. E., Gadgil, S. & Surendran, S. 1999 Improved weather and seasonal climate forecasts from multimodel superensemble. *Science* **285** (5433), 1548–1550. doi:10.1126/science.285.5433.1548.

Krstanovic, P. F. & Singh, V. P. 1991a A univariate model for long-term streamflow forecasting. 1. Development. *Stochastic Hydrology and Hydraulics* **5** (3), 173–188. doi:10.1007/BF01544056.

Krstanovic, P. F. & Singh, V. P. 1991b A univariate model for long-term streamflow forecasting. 2. Application. *Stochastic Hydrology and Hydraulics* **5** (3), 189–205. doi:10.1007/BF01544057.

Kumar, V. & Panu, U. 1997 Predictive assessment of severity of agricultural droughts based on Agro-climatic factors. *Journal of the American Water Resources Association* **33** (6), 1255–1264. 10.1111/j.1752-1688.1997.tb03550.x.

Kumar, K. K., Rajagopalan, B. & Cane, M. A. 1999 On the weakening relationship between the Indian monsoon and ENSO. *Science* **284** (5423), 2156–2159. doi:10.1126/science.284.5423.2156.

Kumar, A., Chen, M., Hoerling, M. & Eischeid, J. 2013 Do extreme climate events require extreme forcings? *Geophysical Research Letters* **40** (13), 3440–3445. doi:10.1002/grl.50657.

Larter, M., Pfautsch, S., Domec, J. C., Trueba, S., Nagalingum, N. & Delzon, S. 2017 Aridity drove the evolution of extreme embolism resistance and the radiation of conifer genus Callitris. *New Phytologist* **215** (1), 97–112. doi:10.1111/nph.14545.

Lee, T. & Salas, J. D. 2011 Copula-based stochastic simulation of hydrological data applied to Nile River flows. *Hydrology Research* **42** (4), 318–330. doi:10.2166/nh.2011.085.

Li, B. L., Wu, H. I. & Zou, G. 2000 Self-thinning rule: a causal interpretation from ecological field theory. *Ecological Modelling* **132** (1–2), 167–173. doi:10.1016/S0304-3800(00)00313-6.

Li, H., Luo, L., Wood, E. F. & Schaake, J. 2009 The role of initial conditions and forcing uncertainties in seasonal hydrologic

forecasting. *Journal of Geophysical Research: Atmospheres* **114** (D4). doi:10.1029/2008JD010969.

Li, Z., Rosenfeld, D. & Fan, J. 2017. Aerosols and their impact on radiation, clouds, precipitation, and severe weather events. In: *Oxford Research Encyclopedia of Environmental Science*. Oxford University Press, New York, USA. doi:10.1093/acrefore/9780199389414.013.126.

Lin, G. F. & Wu, M. C. 2009 A hybrid neural network model for typhoon-rainfall forecasting. *Journal of Hydrology* **375** (3–4), 450–458. doi:10.1016/j.jhydrol.2009.06.047.

Liu, Z. & Alexander, M. 2007 Atmospheric bridge, oceanic tunnel, and global climatic teleconnections. *Reviews of Geophysics* **45** (2). doi:10.1029/2005RG000172.

Liu, W. T. & Juárez, R. N. 2001 ENSO drought onset prediction in northeast Brazil using NDVI. *International Journal of Remote Sensing* **22** (17), 3483–3501. doi:10.1080/01431160010006430.

Lohani, V. K. & Loganathan, G. V. 1997 An early warning system for drought management using the plamer drought index. *Journal of the American Water Resources Association* **33** (6), 1375–1386. doi:10.1111/j.1752-1688.1997.tb03560.x.

Lorenz, D. J., Otkin, J. A., Svoboda, M., Hain, C. R. & Zhong, Y. 2018 Forecasting rapid drought intensification using the Climate Forecast System (CFS). *Journal of Geophysical Research: Atmospheres* **123** (16), 8365–8373. doi:10.1029/2018JD028880.

Ma, F., Ye, A., Deng, X., Zhou, Z., Liu, X., Duan, Q., Xu, J., Miao, C., Di, Z. & Gong, W. 2016 Evaluating the skill of NMME seasonal precipitation ensemble predictions for 17 hydroclimatic regions in continental China. *International Journal of Climatology* **36** (1), 132–144. doi:10.1002/joc.4333.

Ma, F., Ye, A. & Duan, Q. 2019 Seasonal drought ensemble predictions based on multiple climate models in the upper Han River Basin, China. *Climate Dynamics* **53** (12), 7447–7460. doi:10.1007/s00382-017-3577-1.

Madadgar, S. & Moradkhani, H. 2013 A Bayesian framework for probabilistic seasonal drought forecasting. *Journal of Hydrometeorology* **14** (6), 1685–1705. doi:10.1175/JHM-D-13-010.1.

Madadgar, S. & Moradkhani, H. 2014 Spatio-temporal drought forecasting within Bayesian networks. *Journal of Hydrology* **512**, 134–146. doi:10.1016/j.jhydrol.2014.02.0390022-1694.

Madadgar, S., AghaKouchak, A., Shukla, S., Wood, A. W., Cheng, L., Hsu, K. L. & Svoboda, M. 2016 A hybrid statistical-dynamical framework for meteorological drought prediction: application to the southwestern United States. *Water Resources Research* **52** (7), 5095–5110. doi:10.1002/2015WR018547.

Mahanama, S., Livneh, B., Koster, R., Lettenmaier, D. & Reichle, R. 2012 Soil moisture, snow, and seasonal streamflow forecasts in the United States. *Journal of Hydrometeorology* **13** (1), 189–203. doi:10.1175/JHM-D-11-046.1.

Maity, R. & Nagesh Kumar, D. 2008 Probabilistic prediction of hydroclimatic variables with nonparametric quantification of uncertainty. *Journal of Geophysical Research: Atmospheres* **113** (D14). doi:10.1029/2008JD009856.

Martin-StPaul, N., Delzon, S. & Cochard, H. 2017 Plant resistance to drought depends on timely stomatal closure. *Ecology Letters* **20** (11), 1437–1447. doi:10.1111/ele.12851.

Maurer, E. P., Lettenmaier, D. P. & Mantua, N. J. 2004 Variability and potential sources of predictability of North American runoff. *Water Resources Research* **40** (9). doi:10.1029/2003WR002789.

McCabe, G. J. & Dettinger, M. D. 1999 Decadal variations in the strength of ENSO teleconnections with precipitation in the western United States. *International Journal of Climatology: Journal of the Royal Meteorological Society* **19** (13), 1399–1410. doi:10.1002/(SICI)1097-0088(19991115)19:13<1399::AID-JOC457>3.0.CO;2-A.

McCabe, G. J., Palecki, M. A. & Betancourt, J. L. 2004 Pacific and Atlantic Ocean influences on multidecadal drought frequency in the United States. *Proceedings of the National Academy of Sciences* **101** (12), 4136–4141. doi:10.1073/pnas.0306738101.

McCabe, G. J., Betancourt, J. L. & Hidalgo, H. G. 2007 Associations of decadal to multidecadal sea-surface temperature variability with Upper Colorado River Flow. *Journal of the American Water Resources Association* **43** (1), 183–192. doi:10.1111/j.1752-1688.2007.00015.x.

McDowell, N. G. 2011 Mechanisms linking drought, hydraulics, carbon metabolism, and vegetation mortality. *Plant Physiology* **155** (3), 1051–1059. doi:10.1104/pp.110.170704.

McDowell, N., Pockman, W. T., Allen, C. D., Breshears, D. D., Cobb, N., Kolb, T., Plaut, J., Sperry, J., West, A., Williams, D. G. & Yepez, E. A. 2008 Mechanisms of plant survival and mortality during drought: why do some plants survive while others succumb to drought? *New Phytologist* **178** (4), 719–739. doi:10.1111/j.1469-8137.2008.02436.x.

McDowell, N. G., Williams, A. P., Xu, C., Pockman, W. T., Dickman, L. T., Sevanto, S. & Ogee, J. 2016 Multi-scale predictions of massive conifer mortality due to chronic temperature rise. *Nature Climate Change* **6** (3), 295. doi:10.1038/nclimate2873.

McKee, T. B., Doesken, N. J. & Kleist, J. 1993 The relationship of drought frequency and duration to time scales. In: *Proceedings of the 8th Conference on Applied Climatology, 17(22), 179–183*. American Meteorological Society, Boston, MA.

Mette, T., Albrecht, A., Ammer, C., Biber, P., Kohnle, U. & Pretzsch, H. 2009 Evaluation of the forest growth simulator SILVA on dominant trees in mature mixed Silver fir–Norway spruce stands in South-West Germany. *Ecological Modelling* **220** (13–14), 1670–1680. doi:10.1016/j.ecolmodel.2009.03.018.

Mishra, A. K. & Desai, V. R. 2005 Drought forecasting using stochastic models. *Stochastic Environmental Research and Risk Assessment* **19** (5), 326–339. doi:10.1007/s00477-005-0238-4.

Mishra, A. K. & Desai, V. R. 2006 Drought forecasting using feed-forward recursive neural network. *ecological Modelling* **198** (1–2), 127–138. doi:10.1016/j.ecolmodel.2006.04.017.

Mishra, A. K. & Singh, V. P. 2010 A review of drought concepts. *Journal of Hydrology* **391** (1–2), 202–216. doi:10.1016/j.jhydrol.2010.07.012.

Mishra, A. K. & Singh, V. P. 2011 Drought modeling–A review. *Journal of Hydrology* **403** (1–2), 157–175. doi:10.1016/j.jhydrol.2011.03.049.

Mishra, A. K., Desai, V. R. & Singh, V. P. 2007 Drought forecasting using a hybrid stochastic and neural network model. *Journal of Hydrologic Engineering* **12** (6), 626–638. doi:10.1061/(ASCE)1084-0699(2007)12:6(626).

Mishra, A. K., Singh, V. P. & Desai, V. R. 2009 Drought characterization: a probabilistic approach. *Stochastic Environmental Research and Risk Assessment* **23** (1), 41–55. doi:10.1007/s00477-007-0194-2.

Mo, K. C. & Lettenmaier, D. P. 2014 Hydrologic prediction over the conterminous United States using the national multi-model ensemble. *Journal of Hydrometeorology* **15** (4), 1457–1472. doi:10.1175/JHM-D-13-0197.1.

Mo, K. C. & Lyon, B. 2015 Global meteorological drought prediction using the North American multi-model ensemble. *Journal of Hydrometeorology* **16** (3), 1409–1424. doi:10.1175/JHM-D-14-0192.1.

Mo, K. C. & Schemm, J. E. 2008 Relationships between ENSO and drought over the southeastern United States. *Geophysical Research Letters* **35** (15). doi:10.1029/2008GL034656.

Moghimi, M. M., Zarei, A. R. & Mahmoudi, M. R. 2019 Seasonal drought forecasting in arid regions, using different time series models and RDI index. *Journal of Water and Climate Change*. doi:10.2166/wcc.2019.009.

Mohseni, O., Stefan, H. G. & Erickson, T. R. 1998 A nonlinear regression model for weekly stream temperatures. *Water Resources Research* **34** (10), 2685–2692. doi:10.1029/98WR01877.

Molteni, F., Stockdale, T., Balmaseda, M., Balsamo, G., Buizza, R., Ferranti, L., Magnusson, L., Mogensen, K., Palmer, T. & Vitart, F. 2011 *The new ECMWF Seasonal Forecast System (System 4) (Vol. 49)*. European Centre for Medium-Range Weather Forecasts, Reading, UK.

Montaseri, M., Amirataee, B. & Rezaie, H. 2018 New approach in bivariate drought duration and severity analysis. *Journal of Hydrology* **559**, 166–181. doi:10.1016/j.jhydrol.2018.02.018.

Moorcroft, P. R., Hurtt, G. C. & Pacala, S. W. 2001 A method for scaling vegetation dynamics: the ecosystem demography model (ED). *Ecological Monographs* **71** (4), 557–586. doi:10.1890/0012-9615(2001)071[0557:AMFSVD]2.0.CO;2.

Mukherjee, S., Mishra, A. & Trenberth, K. E. 2018 Climate change and drought: a perspective on drought indices. *Current Climate Change Reports* **4** (2), 145–163. doi:10.1007/s40641-018-0098-x.

Munns, R. 2002 Comparative physiology of salt and water stress. *Plant, Cell & Environment* **25** (2), 239–250. doi:10.1046/j.0016-8025.2001.00808.x.

Nam, W. H., Hayes, M. J., Svoboda, M. D., Tadesse, T. & Wilhite, D. A. 2015 Drought hazard assessment in the context of climate change for South Korea. *Agricultural Water Management* **160**, 106–117. doi:10.1016/j.agwat.2015.06.029.

Newman, M., Compo, G. P. & Alexander, M. A. 2003 ENSO-forced variability of the Pacific decadal oscillation. *Journal of Climate* **16** (23), 3853–3857. doi:10.1175/1520-0442(2003)016<3853:EVOTPD>2.0.CO;2.

Nobre, C. A., Sellers, P. J. & Shukla, J. 1991 Amazonian deforestation and regional climate change. *Journal of Climate* **4** (10), 957–988. doi:10.1175/1520-0442(1991)004<0957:ADARCC>2.0.CO;2.

Özger, M., Mishra, A. K. & Singh, V. P. 2012 Long lead time drought forecasting using a wavelet and fuzzy logic combination model: a case study in Texas. *Journal of Hydrometeorology* **13** (1), 284–297. doi:10.1175/JHM-D-10-05007.1.

Padmanabhan, G. & Rao, A. R. 1988 Maximum entropy spectral analysis of hydrologic data. *Water Resources Research* **24** (9), 1519–1533. doi:10.1029/WR024i009p01519.

Pan, M. & Wood, E. F. 2006 Data assimilation for estimating the terrestrial water budget using a constrained ensemble Kalman filter. *Journal of Hydrometeorology* **7** (3), 534–547. doi:10.1175/JHM495.1.

Palmer, W. C. 1965 *Meteorological Drought*. Res. Pap, 45, US Weather Bureau, Washington, DC.

Palmer, T. N., Alessandri, A., Andersen, U., Cantelaube, P., Davey, M., Delécluse, P., Déqué, M., Diez, E., Doblas-Reyes, F. J., Feddersen, H. & Graham, R. 2004 Development of a European multimodel ensemble system for seasonal-to-interannual prediction (DEMETER). *Bulletin of the American Meteorological Society* **85** (6), 853–872. doi:10.1175/BAMS-85-6-853.

Rajsekhar, D., Singh, V. P. & Mishra, A. K. 2015 Integrated drought causality, hazard, and vulnerability assessment for future socioeconomic scenarios: an information theory perspective. *Journal of Geophysical Research: Atmospheres* **120** (13), 6346–6378. doi:10.1002/2014JD022670.

Reddy, M. J. & Singh, V. P. 2014 Multivariate modeling of droughts using copulas and meta-heuristic methods. *Stochastic Environmental Research and Risk Assessment* **28** (3), 475–489. doi:10.1007/s00477-013-0766-2.

Reyer, C., Lasch-Born, P., Suckow, F., Gutsch, M., Murawski, A. & Pilz, T. 2014 Projections of regional changes in forest net primary productivity for different tree species in Europe driven by climate change and carbon dioxide. *Annals of Forest Science* **71** (2), 211–225. doi:10.1007/s13595-013-0306-8.

Roman, D. T., Novick, K. A., Brzostek, E. R., Dragoni, D., Rahman, F. & Phillips, R. P. 2015 The role of isohydric and anisohydric species in determining ecosystem-scale response to severe drought. *Oecologia* **179** (3), 641–654. doi:10.1007/s00442-015-3380-9.

Saha, S., Moorthi, S., Wu, X., Wang, J., Nadiga, S., Tripp, P., Behringer, D., Hou, Y. T., Chuang, H. Y., Iredell, M. & Ek, M. 2014 The NCEP climate forecast system version 2.

Journal of Climate **27** (6), 2185–2208. doi:10.1175/JCLI-D-12-00823.1.

Samantaray, A. K., Singh, G., Ramadas, M. & Panda, R. K. 2019 Drought hotspot analysis and risk assessment using probabilistic drought monitoring and severity–duration–frequency analysis. *Hydrological Processes* **33** (3), 432–449. doi:10.1002/hyp.13337.

Scheff, J. 2018 Drought indices, drought impacts, CO_2, and warming: a historical and geologic perspective. *Current Climate Change Reports* **4** (2), 202–209. doi:10.1007/s40641-018-0102-5.

Scheller, R. M. & Mladenoff, D. J. 2004 A forest growth and biomass module for a landscape simulation model, LANDIS: design, validation, and application. *Ecological Modelling* **180** (1), 211–229. doi:10.1016/j.ecolmodel.2004.01.022.

Schepen, A. & Wang, Q. J. 2015 Model averaging methods to merge operational statistical and dynamic seasonal streamflow forecasts in Australia. *Water Resources Research* **51** (3), 1797–1812. doi:10.1002/2014WR016163.

Schepen, A., Wang, Q. J. & Robertson, D. E. 2014 Seasonal forecasts of Australian rainfall through calibration and bridging of coupled GCM outputs. *Monthly Weather Review* **142** (5), 1758–1770. doi:10.1175/MWR-D-13-00248.1.

Schubert, S. D., Stewart, R. E., Wang, H., Barlow, M., Berbery, E. H., Cai, W., Hoerling, M. P., Kanikicharla, K. K., Koster, R. D., Lyon, B. & Mariotti, A. 2016 Global meteorological drought: a synthesis of current understanding with a focus on SST drivers of precipitation deficits. *Journal of Climate* **29** (11), 3989–4019. doi:10.1175/JCLI-D-15-0452.1.

Seager, R., Kushnir, Y., Herweijer, C., Naik, N. & Velez, J. 2005 Modeling of tropical forcing of persistent droughts and pluvials over western North America: 1856–2000. *Journal of Climate* **18** (19), 4065–4088. doi:10.1175/JCLI3522.1.

Seager, R., Hoerling, M., Schubert, S. D., Wang, H., Lyon, B., Kumar, A., Nakamura, J. & Henderson, N. 2014 *Causes and Predictability of the 2011–14 California Drought: Assessment Report*.

Sehgal, V. & Sridhar, V. 2019 Watershed-scale retrospective drought analysis and seasonal forecasting using multi-layer, high-resolution simulated soil moisture for southeastern US. *Weather and Climate Extremes* **23**, 100191. doi:10.1016/j.wace.2018.100191.

Sehgal, V., Sridhar, V., Juran, L. & Ogejo, J. 2018 Integrating climate forecasts with the soil and water assessment tool (SWAT) for high-Resolution hydrologic simulations and forecasts in the Southeastern US. *Sustainability* **10** (9), 3079. doi:10.3390/su10093079.

Shafiee-Jood, M., Cai, X., Chen, L., Liang, X. Z. & Kumar, P. 2014 Assessing the value of seasonal climate forecast information through an end-to-end forecasting framework: application to US 2012 drought in central Illinois. *Water Resources Research* **50** (8), 6592–6609. doi:10.1002/2014WR015822.

Sharma, T. C. & Panu, U. S. 2012 Prediction of hydrological drought durations based on Markov chains: case of the Canadian prairies. *Hydrological Sciences Journal* **57** (4), 705–722. doi:10.1080/02626667.2012.672741.

Sheffield, J. & Wood, E. F. 2012 *Drought: Past Problems and Future Scenarios*. Routledge, London, UK.

Shukla, S. & Lettenmaier, D. P. 2011 Seasonal hydrologic prediction in the United States: understanding the role of initial hydrologic conditions and seasonal climate forecast skill. *Hydrology and Earth System Sciences* **15** (11), 3529–3538. doi:10.5194/hess-15-3529-2011.

Shukla, S., Sheffield, J., Wood, E. F. & Lettenmaier, D. P. 2013 On the sources of global land surface hydrologic predictability. *Hydrology and Earth System Sciences*. doi:10.5194/hess-17-2781-2013.

Shumway, R. H. & Stoffer, D. S. 2017 *Time Series Analysis and its Applications: with R Examples*. Springer, New York, USA.

Singh, V. P. 1997 The use of entropy in hydrology and water resources. *Hydrological Processes* **11** (6), 587–626. doi:10.1002/(SICI)1099-1085(199705)11:6<587::AID-HYP479>3.0.CO;2-P.

Singh, V. P. 2011 Hydrologic synthesis using entropy theory. *Journal of Hydrologic Engineering* **16** (5), 421–433. doi:10.1061/(ASCE)HE.1943-5584.0000332.

Smith, B., Prentice, I. C. & Sykes, M. T. 2001 Representation of vegetation dynamics in the modelling of terrestrial ecosystems: comparing two contrasting approaches within European climate space. *Global Ecology and Biogeography* **10** (6), 621–637. doi:10.1046/j.1466-822X.2001.t01-1-00256.x.

Sperry, J. S., Adler, F. R., Campbell, G. S. & Comstock, J. P. 1998 Limitation of plant water use by rhizosphere and xylem conductance: results from a model. *Plant, Cell & Environment* **21** (4), 347–359. doi:10.1046/j.1365-3040.1998.00287.x.

Sperry, J. S., Hacke, U. G., Oren, R. & Comstock, J. P. 2002 Water deficits and hydraulic limits to leaf water supply. *Plant, Cell & Environment* **25** (2), 251–263. doi:10.1046/j.0016-8025.2001.00799.x.

Strazzo, S., Collins, D. C., Schepen, A., Wang, Q. J., Becker, E. & Jia, L. 2019 Application of a hybrid statistical–dynamical system to seasonal prediction of North American temperature and precipitation. *Monthly Weather Review* **147** (2), 607–625. doi:10.1175/MWR-D-18-0156.1.

Sud, Y. C., Sellers, P. J., Mintz, Y., Chou, M. D., Walker, G. K. & Smith, W. E. 1990 Influence of the biosphere on the global circulation and hydrologic cycle – A GCM simulation experiment. *Agricultural and Forest Meteorology* **52** (1–2), 133–180. doi:10.1016/0168-1923(90)90104-E.

Sutanto, S. J., van der Weert, M., Wanders, N., Blauhut, V. & Van Lanen, H. A. 2019 Moving from drought hazard to impact forecasts. *Nature Communications* **10** (1), 1–7. doi:10.1038/s41467-019-12840-z.

Swain, D. L., Tsiang, M., Haugen, M., Singh, D., Charland, A., Rajaratnam, B. & Diffenbaugh, N. S. 2014 The extraordinary California drought of 2013/2014: character, context, and the role of climate change. *Bulletin of the American Meteorological Society* **95** (9), S3–S7.

Thilakarathne, M. & Sridhar, V. 2017 Characterization of future drought conditions in the Lower Mekong River Basin. *Weather and Climate Extremes* **17**, 47–58. doi:10.1016/j.wace.2017.07.004.

Thomas, D. S. G. & Middleton, N. J. 1993 Salinization: new perspectives on a major desertification issue. *Journal of Arid Environments* **24** (1), 95–105. doi:10.1006/jare.1993.1008.

Thrippleton, T., Hülsmann, L., Cailleret, M. & Bugmann, H. 2019 Projecting forest dynamics across Europe: potentials and pitfalls of empirical mortality algorithms. *Ecosystems* 1–16. doi:10.1007/s10021-019-00397-3.

Thyer, M., Frost, A. J. & Kuczera, G. 2006 Parameter estimation and model identification for stochastic models of annual hydrological data: is the observed record long enough? *Journal of Hydrology* **330** (1–2), 313–328. doi:10.1016/j.jhydrol.2006.03.029.

Trenberth, K. E., Dai, A., Van Der Schrier, G., Jones, P. D., Barichivich, J., Briffa, K. R. & Sheffield, J. 2014 Global warming and changes in drought. *Nature Climate Change* **4** (1), 17–22. doi:10.1038/nclimate2067.

Turco, M., Ceglar, A., Prodhomme, C., Soret, A., Toreti, A. & Francisco, J. D. R. 2017 Summer drought predictability over Europe: empirical versus dynamical forecasts. *Environmental Research Letters* **12** (8), 084006. doi:10.1088/1748-9326/aa7859.

Vanli, N. D. & Kozat, S. S. 2014 A comprehensive approach to universal piecewise nonlinear regression based on trees. *IEEE Transactions on Signal Processing* **62** (20), 5471–5486.

van Mantgem, P. J., Stephenson, N. L., Byrne, J. C., Daniels, L. D., Franklin, J. F., Fulé, P. Z., Harmon, M. E., Larson, A. J., Smith, J. M., Taylor, A. H. & Veblen, T. T. 2009 Widespread increase of tree mortality rates in the western United States. *Science* **323** (5913), 521–524. doi:10.1126/science.1165000.

van Nieuwstadt, M. G. & Sheil, D. 2005 Drought, fire and tree survival in a Borneo rain forest, East Kalimantan, Indonesia. *Journal of Ecology* **93** (1), 191–201. doi:10.1111/j.1365-2745.2004.00954.x.

Vanoni, M., Cailleret, M., Hülsmann, L., Bugmann, H. & Bigler, C. 2019 How do tree mortality models from combined tree-ring and inventory data affect projections of forest succession? *Forest Ecology and Management* **433**, 606–617. Doi:10.1016/j.foreco.2018.11.042.

Vicente-Serrano, S. M., Beguería, S. & López-Moreno, J. I. 2010 A multiscalar drought index sensitive to global warming: the standardized precipitation evapotranspiration index. *Journal of Climate* **23** (7), 1696–1718. doi:10.1175/2009JCLI2909.1.

Wanders, N. & Wood, E. F. 2016 Improved sub-seasonal meteorological forecast skill using weighted multi-model ensemble simulations. *Environmental Research Letters* **11** (9), 094007. doi:10.1088/1748-9326/11/9/094007.

Wang, H. & Schubert, S. 2014 Causes of the extreme dry conditions over California during early 2013, in Explaining Extreme Events of 2013. *Bulletin of the American Meteorological Society* **95** (9), S7–S10. doi:10.1175/1520-0477-95.9.S1.1.

Wang, S. Y., Hipps, L., Gillies, R. R. & Yoon, J. H. 2014 Probable causes of the abnormal ridge accompanying the 2013–2014 California drought: ENSO precursor and anthropogenic warming footprint. *Geophysical Research Letters* **41** (9), 3220–3226. doi:10.1002/2014GL059748.

West, A. G., Hultine, K. R., Sperry, J. S., Bush, S. E. & Ehleringer, J. R. 2008 Transpiration and hydraulic strategies in a piñon–juniper woodland. *Ecological Applications* **18** (4), 911–927. doi:10.1890/06-2094.1.

Wilhite, D. A. 2005 *Drought and Water Crises: Science, Technology, and Management Issues*. CRC Press, Boca Raton, USA.

Williams, A. P., Allen, C. D., Millar, C. I., Swetnam, T. W., Michaelsen, J., Still, C. J. & Leavitt, S. W. 2010 Forest responses to increasing aridity and warmth in the southwestern United States. *Proceedings of the National Academy of Sciences* **107** (50), 21289–21294. doi:10.1073/pnas.0914211107.

Williams, A. P., Allen, C. D., Macalady, A. K., Griffin, D., Woodhouse, C. A., Meko, D. M., Swetnam, T. W., Rauscher, S. A., Seager, R., Grissino-Mayer, H. D. & Dean, J. S. 2013 Temperature as a potent driver of regional forest drought stress and tree mortality. *Nature Climate Change* **3** (3), 292–297. doi:10.1038/nclimate1693.

Williams, A. P., Seager, R., Abatzoglou, J. T., Cook, B. I., Smerdon, J. E. & Cook, E. R. 2015 Contribution of anthropogenic warming to California drought during 2012–2014. *Geophysical Research Letters* **42** (16), 6819–6828. doi:10.1002/2015GL064924.

Wong, G., Lambert, M. F., Leonard, M. & Metcalfe, A. V. 2009 Drought analysis using trivariate copulas conditional on climatic states. *Journal of Hydrologic Engineering* **15** (2), 129–141. doi:10.1061/(ASCE)HE.1943-5584.0000169.

Wood, A. W. & Lettenmaier, D. P. 2008 An ensemble approach for attribution of hydrologic prediction uncertainty. *Geophysical Research Letters* **35** (14). doi:10.1029/2008GL034648.

Wood, E. F., Schubert, S. D., Wood, A. W., Peters-Lidard, C. D., Mo, K. C., Mariotti, A. & Pulwarty, R. S. 2015 Prospects for advancing drought understanding, monitoring, and prediction. *Journal of Hydrometeorology* **16** (4), 1636–1657. doi:10.1175/JHM-D-14-0164.1.

Worster, D. 2004 *Dust Bowl: the Southern Plains in the 1930s*. Oxford University Press, New York, USA.

Xiao, M., Zhang, Q. & Singh, V. P. 2015 Influences of ENSO, NAO, IOD and PDO on seasonal precipitation regimes in the Yangtze River basin, China. *International Journal of Climatology* **35** (12), 3556–3567. doi:10.1002/joc.4228.

Xiao, M., Zhang, Q., Singh, V. P. & Chen, X. 2017 Probabilistic forecasting of seasonal drought behaviors in the Huai River basin, China. *Theoretical and Applied Climatology* **128** (3–4), 667–677. doi:10.1007/s00704-016-1733-x.

Xu, L., Chen, N., Zhang, X. & Chen, Z. 2018 An evaluation of statistical, NMME and hybrid models for drought prediction in China. *Journal of Hydrology* **566**, 235–249. doi:10.1016/j.jhydrol.2018.09.020.

Yang, J., Chang, J., Wang, Y., Li, Y., Hu, H., Chen, Y., Huang, Q. & Yao, J. 2018 Comprehensive drought characteristics analysis

based on a nonlinear multivariate drought index. *Journal of Hydrology* **557**, 651–667. doi:10.1016/j.jhydrol.2017.12.055.

Yeh, S. W., Cai, W., Min, S. K., McPhaden, M. J., Dommenget, D., Dewitte, B., Collins, M., Ashok, K., An, S. I., Yim, B. Y. & Kug, J. S. 2018 ENSO atmospheric teleconnections and their response to greenhouse gas forcing. *Reviews of Geophysics* **56** (1), 185–206. doi:10.1002/2017RG000568.

Yevjevich, V. M. 1967 Objective approach to definitions and investigations of continental hydrologic droughts. *Hydrology papers No. 23*. Colorado State University, Fort Collins, USA.

Yoda, K. 1963 Self-thinning in overcrowded pure stands under cultivated and natural conditions (Intraspecific competition among higher plants. XI). *Journal of the Institute of Polytechnics, Osaka City University. Series D* **14**, 107–129.

Yuan, X. & Wood, E. F. 2013 Multimodel seasonal forecasting of global drought onset. *Geophysical Research Letters* **40** (18), 4900–4905. doi:10.1002/grl.50949.

Yuan, X., Roundy, J. K., Wood, E. F. & Sheffield, J. 2015 Seasonal forecasting of global hydrologic extremes: system development and evaluation over GEWEX basins. *Bulletin of the American Meteorological Society* **96** (11), 1895–1912. doi:10.1175/BAMS-D-14-00003.1.

Zhang, L. & Singh, V. P. 2019 *Copulas and Their Applications in Water Resources Engineering*. Cambridge University Press.

Zhang, Q., Xiao, M., Singh, V. P. & Chen, X. 2013 Copula-based risk evaluation of hydrological droughts in the East River basin, China. *Stochastic Environmental Research and Risk Assessment* **27** (6), 1397–1406. doi:10.1007/s00477-012-0675-9.

First received 4 November 2019; accepted in revised form 24 March 2020. Available online 13 April 2020